Draft Manuscript for Review

"Nephroprotective Potential of Ginger, Diosmin, and Their Combination on Induced Diabetic Nephropathy in a Rat Model: Light and Electron Microscopic Observations"

Journal:	Egyptian Journal of Histology
Manuscript ID:	EJH-2407-2109 (R3)
Manuscript Title:	Nephroprotective Potential of Ginger, Diosmin, and Their Combination on Induced Diabetic Nephropathy in a Rat Model: Light and Electron Microscopic Observations

Nephroprotective Potential of Ginger, Diosmin, and Their Combination on Induced Diabetic Nephropathy in a Rat Model: Light and Electron Microscopic Study

Abstract

Background: Hyperglycemia is a chronic illness that is associated with diabetes. Patients with diabetes have been found to have many alterations in their renal functioning. The aim of this study was to evaluate the potential benefits of diosmin and ginger, either separately or in combination, for diabetic nephropathy that was experimentally produced.

Materials and Methods: Group I, ten rats stood as a control group. All rats (except control group) were given a single intraperitoneal dose of alloxan (150 mg/kg body weight) to induce type 2 diabetes. Group II consisted of ten diabetic rats. Other ten diabetic rats received 100 mg/kg diosmin orally for six weeks as part of Group III. Also other ten diabetic rats; part of Group IV received 400 mg/kg of ginger orally for six weeks. The last ten diabetic rats in Group V received oral treatment for six weeks with ginger (400 mg/kg) and diosmin (100 mg/kg). Rats were sacrificed after the six weeks, and kidney tissue and blood samples were taken for several biochemical analyses. Both an ultrastructural investigation and hemotoxylin and eosin staining were performed. The desmin and Nrf2 immunohistochemical markers were used. There were statistical and morphometric studies performed.

Results: the diosmin plus ginger therapy showed a considerable decrease in blood glucose, urea, and creatinine in contrast to rats with diabetes. After six weeks, there was a noticeable recovery in the levels of malondialdehyde (MDA), catalase (CAT) and superoxide dismutase (SOD). Histopathological analysis verified that group V likewise had apparently normal renal tissue architecture. When compared to the diabetic group, area% of Desmin in group V was much lower, while its area% of Nrf2 was significantly greater.

Conclusion: Ginger treatment alone or in combination with diosmin exhibited more pronounced improvement in diabetic nephropathy.

Keywords: Diosmin; Ginger; Diabetic Nephropathy; Nrf2; Desmin.

Introduction

Diabetes mellitus (DM) is defined by a persistently high blood sugar level coupled with abnormalities in the metabolism of carbohydrates, lipids, and proteins. These abnormalities can be caused by deficiencies in either alter the release of insulin, the function of insulin, or both [(1)]. Elevated glucose concentrations in the cellar area cause oxidative stress because they enhance the formation of free radicals and lower natural antioxidant defenses. The development of diabetic problems is closely linked to oxidative stress, which is primarily caused by the production of free radicals that cause tissue damage. Diabetes is a major contributor to kidney failure, coronary heart disease, stroke, lower limb amputation, and blindness [(2)]. Various insulin formulations and oral hypoglycemic drugs, such as sulfonlyureas, are being utilized to treat Type 2 diabetes. These medications provide only moderate protection against renal advancement, despite their substantial benefits in managing hyperglycemia [(3)].

Ginger, or Zingiber officinale roscoe, is a member of the Zingiberaceae family and is a common spice in cooking. Zingiber officinale has major biologically active chemicals such paradols, shogaols, and gingerols, but a chemical examination reveals that it contains over 400 distinct compounds. Common illnesses including headaches, nausea, and colds are frequently treated with ginger alone [(4)]. Zingiber officinale has been shown to have a variety of therapeutic effects in mouse experiments, including anti-emetic properties in cancer treatment [(5)] and anti-inflammatory properties against inflammation-related disorders such colitis [(6)]. Many in vitro and in vivo studies have looked at ginger's and its compounds' anti-oxidative properties. The results showed that ginger decreased induced lipid peroxidation and markedly increased serum glutathione and antioxidant enzyme levels [(7)].

Diosmin (diosmetin 7-O-rutinoside, C28H32O15) is a naturally present flavone glycoside that is commonly found in citrus trees that are part of the rutaceae family, which includes tangerines (Citrus reticulata). Its molecular weight is 608.549 g/mol. It presents significant pharmacological properties like anti-oxidant, anti-inflammatory, anti-hyperglycemic, anti-mutagenic, anti-rheumatic, and anti-allergic properties [(8)]. Diosmin has been shown in a recent study to protect against cadmium-

induced liver damage [9], cerebral ischemia [10] and memory impairment brought on by traumatic brain damage [11].

The current study aimed to: assess zingerone's protective effect against induced-diabetes; assess Diosmin's protective effect against diabetes-mediated nephropathy; assess the protective effect of their combination; and compare the renoprotective effect of both drugs with induced-diabetes through changes in the kidney's histology.

Materials and Methods

Animals

we used fifty adult male albino rats, ranging 200–250 g of weight that we bought from the Faculty of Medicine's animal house at Cairo University. The rats were housed in standard conditions, 24 ± 10°C, 65 ± 5% humidity, and a reversible 12-hour light/dark cycle. All rats had access to clean water to drink and eat. The Benha Ethics Committee's approval was granted in compliance with the rules of ethics for experimental animals (Ethical Approval NO.: RC 16-9-2023).

Chemicals

Alloxan monohydrate powder (Cat no. A7413- 10g) was supplied from Sigma-Aldrich Chemie GmbH.

Diosmin powder (CAS no. 520-27-4) was obtained from Sigma-Aldrich Chemie GmbH.

Ginger was obtained from MEPACO Company (Sharquia, Egypt) as 30 tablets (each tablet has 400 mg of ginger rhizome powder).

Experimental design

Five experimental groups were randomly selected from among fifty rats; each group was included:

Group I (control group): consisted of ten rats. The rats were separated into five subgroups, each consisting of two rats as follows:

Subgroup Ia: rats were given a standard diet for six weeks.

Subgroup Ib: rats was injected intraperitoneally with 1 ml of normal saline as single dose equal the amount used to dissolve alloxan monohydrate.

Subgroup Ic: rats were given diosmin 100 mg/kg (dissolved in saline in total volume of 1 ml) orally through gastric gavage every day for six weeks [12]

Subgroup Id: rats were received with 400 mg/kg of ginger (dissolved in saline in total volume of 1 ml) orally every day for six weeks through gastric gavage [13].

Subgroup Ie: rats were given diosmin 100 mg/kg (dissolved in saline in total volume of 1 ml) in addition to 400 mg/kg of ginger (dissolved in saline in total volume of 1 ml) orally by gastric gavage for six weeks.

Group II (Diabetic group):

All of the other forty rats were used to induce Diabetes. Rats, that had been starved all night, were given 150 mg/kg of alloxan monohydrate (dissolved in saline in total volume of 1 ml) through an intraperitoneal injection. The blood glucose monitoring equipment (SD biosensor Inc. Korea) was used to measure the blood glucose levels from the tail vein after a fast of 72 hours. Rats that tested for blood glucose and recorded more than 250 mg/dl were chosen to complete this study. Since alloxan induces fatal hypoglycemia six hours after injection, the rats were fed a 20% glucose solution for the next twenty-four hours in 50 ml small water feeding bottles [14]. After that, the rats with developed diabetes were fed a regular diet for a period of six weeks.

As a result, ten diabetic rats were housed for six weeks without receiving any medication and considered as diabetic group as chronic hyperglycemia is typically the precursor to diabetic nephropathy [14]. The remaining thirty diabetic rats were used in group III, IV and V.

Group III (Dio group): ten diabetic rats were received diosmin treatment (100 mg/kg orally every day for six weeks as in subgroup Ic) after diabetes was well established (induction of diabetes by alloxan as mentioned in group II).

Group IV (Gin group): ten diabetic rats were received ginger (400 mg/kg orally every day for six weeks as in subgroub Id) after diabetes was well established (induction of diabetes by alloxan as mentioned in group II).

Group V (D+G group): ten diabetic rats received combination of ginger and diosmin in a dose as in subgroup Ie after diabetes was well established (induction of diabetes by alloxan as mentioned in group II).

The rats were anesthetized at the end of the trial by breathing in diethyl ether. After the rats were sacrificed, blood sample (5 ml.) was collected from tail vein of each rat in the plain tube for biochemical analysis to determine blood glucose levels and renal functions. Specimens were prepared for light and electron microscopy investigations following kidney dissection.

Biochemical measurements

The blood glucose levels were measured using the blood glucose monitoring equipment. Blood samples were centrifuged for 20 minutes after being allowed to clot for two hours at room temperature. The serum was easily removed and stored at -20 °C. The enzymatic, colorimetric approach was used to determine the urea level [15]. Quantitative reagent kit also used to test creatinine level [16]. All the kits were purchased from Biodiagnostics Co. (Cairo, Egypt).

Oxidative stress and antioxidant biomarkers

After being dissected, sliced frozen kidneys were mixed with distilled water until smooth. A clear kidney homogenate supernatant was used to identify antioxidant and oxidative stress indicators.

Considering that the quantity of malondialdehyde formed when polyunsaturated fatty acids break down, the MDA (lipid peroxidation) (MDA Elabscience Kit Catalog No. E-EL-0060, USA) was estimated [17]. Additionally, the level of superoxide dismutase activity (SOD antioxidant enzyme) (SOD Elabscience Kit Catalog no. E-EL-R1424, USA) was measured using the Marklund and Marklund approach [18] because pyrogallol inhibits auto-oxidation by catalyzing the breakdown of superoxide. Monitoring the breakdown of hydrogen peroxide enzyme, which is

catalyzed by potassium permanganate, allowed researchers to determine the degree of antioxidant enzyme of CAT (CAT Elabscience Kit Catalog No. E-BC-K031-M, USA) [19].

Histological and immunohistochemical studies

Right kidney specimens were embedded in formalin saline 10% buffer. Paraffin sections ranging in thickness from 5 to 7 μm were arranged and placed on glass slides for staining with H and E [20]. Sections of tissue that had been deparaffinized, were treated with 3% H2O2 for thirty minutes. Following this, they were incubated with anti-Desmin and anti-Nrf2 (Nuclear factor erythroid 2-related factor 2) for one hour at 37 °C as directed by the manufacturer. The method used to complete was taken from Jakkson, & Blqthe [21].

The primary Rabbit Recombinant Monoclonal Desmin antibody was used (ab227651, Abcam [SP138], Waltham, MA, 1:100). Brown color in the cytoplasm of glomerular podocytes served as an indicator of podocyte stress [22]. Nrf2 (PA5-27882, Thermo Fisher Scientific, Rockford, USA, 1:100) is one of oxidative stress response marker that binds to antioxidant response elements in the promoter regions. The positive reaction was brown color in the cytoplasm of renal tubules [23].

In the Anatomy and Embryology department of the Faculty of Medicine at Benha University, H&E and Immunohistochemical sections were examined and captured on camera using a light microscope (Olympus CX 41, Japan) and an attached camera (Olympus E 330, Japan).

Ultrastructural preparations

Left kidney samples of approximately 1 mm^3 were sliced and preserved in a 3% glutaraldehyde–formaldehyde solution for ultrastructural examinations. After being cleaned with PB (pH 7.4), these samples were post-fixed for an hour at 4 °C in 1% isotonic osmium tetroxide post. The sections were processed for electron microscopic analysis. We stained the semi-thin slices with toluidine blue in order to determine the target location. After that, we used glass blades from an ultramicrotome to create ultrathin slices [24]. After staining the specimens with lead citrate and uranyl acetate, we examined the samples under an electron microscope using the JEOL

(JEM-100 SX Akishima, Tokyo, Japan) transmission. It was carried out at the Benha University Faculty of Medicine's Electron Microscopy Unit at the Histology Department.

Statistical analysis

The % area of Desmin and Nrf2 positive expression in the innunohistochemical renal sections at 400× magnification was determined using the Image J software analyzer computer. Using SPSS v28 (IBM Inc., Armonk, NY, USA) for the statistical analysis, All information, including the mean Area (%) of positive immunohistochemistry expression levels of Nrf2 and Desmin in immune stained sections was represented as mean±SD for each group. Also, blood glucose, serum urea and creatinine levels, MDA, SOD and CAT levels were represented as mean±SD for each group .The two groups were compared using the ANOVA (F) test. The qualitative variables were analyzed using the Chi-square test, which were given as frequency and percentage (%). P-values of less than 0.05 and higher than 0.05, respectively, indicated that the results were statistically significant and nonsignificant at that point.

Results

Biochemical measurements

Diabetic group, Dio and Gin groups had significantly increase in glucose levels than group I. Dio, Gin and D+G groups had significantly decreased in glucose levels than Diabetic group. Gin and D+G groups had significantly lower glucose levels than Dio group (table 1).

In comparison to control group, the urea level increased significantly in Dio, Gin and D+G groups. In comparison to Diabetic group, the urea level decreased significantly in in Dio, Gin and D+G groups. In comparison to Dio group, the urea level decreased significantly in in Gin and D+G groups, and it was significantly lower in D+G group when compared to Gin group (table 1).

Diabetic and Dio groups had significantly increased in creatinine levels than control group. In comparison to Diabetic group, the levels of creatinine in Dio, Gin

and D+G groups were significantly decreased. It was significantly decreased in D+G group when compared to Dio group (table 1).

Oxidative stress and antioxidant biomarkers

In comparison to control group, MDA was significantly increased in Diabetic group Dio and Gin groups. MDA in Gin and D+G groups was significantly decreased than in Diabetic group. Furthermore, MDA was significantly increased in Gin group as compared to D+G group and significantly decreased in Gin and D+G groups as compared to Dio group.

In comparison to control group, the SOD levels in Diabetic, Dio, and Gin and D+G groups were significantly reduced. In comparison to Diabetic group, the SOD levels in Gin and D+G groups were significantly increased. SOD level in D+G group was significantly decreased than that of Dio and Gin groups.

In comparison to group I, the levels of catalase in Diabetic and Dio groups were significantly decreased. Gin and D+G groups were significantly increased of catalase than in Diabetic group. Catalase level of D+G group was significantly increased comparing to Dio group.

Hematoxylin and eosin stain

Kidney segment examination of every subgroup in control group produced the identical histological results; hence they were all regarded as a control group. H and E-stained slices of the control group showed the renal tubules and the renal corpuscle in the renal cortex. The renal corpuscle consisted of renal glomeruli, which were surrounded by Bowman's capsule and had a tuft of capillaries. The urinary gap is what separated Bowman's capsule from the glomerulus. A single layer of basic squamous epithelium coated the parietal covering of Bowman's capsule. Cuboidal cells with acidophilic cytoplasm bordered the proximal convoluted tubules (PCT). They had centrally located, vesicular, rounded nuclei. The apical brush borders and poorly defined boundaries were seen in the cells. In the distal convoluted tubules (DCT), the lumen was broad. The cuboidal cells lined DCT and had spherical vesicular nuclei (Figure.1)

However, diabetic group had shrinkage in glomerular capillaries with wide urinary space. The majority of the PCT had dilated lumen and missing of apical brush border. Renal tubules had intraluminal debris, which indicated desquamated cells. Both the proximal and distal tubular cells showed vacuolated cytoplasm (Figure.2).

On the other hand, administration of Diosmin in group III improved glomerular structure and increased Bowman's space. Most likely, some of the renal tubules were normal. Certain tubular cells exhibited dark stained nuclei and cytoplasmic vacuolizations (Figure.3).

The diabetes histological alterations in Gin group improved; there was normal Bowman‘s space and about normal convoluted tubules with some vacuolated cells. Peritubular congested blood vessels were seen (Figure.4). D+G group resembled the control group in most respects with apparently normal of the glomerular capillaries and urinary space. PCT had rounded nuclei with apical brush borders. DCT lined with cubical cells with round nuclei. Congested peritubular blood vessels were observed (Figure.5).

Ultrastructural findings

The glomerular capillaries in sections of control rats were lined with fenestrated endothelial cells with basement membrane. Glomerular basement membrane showed up with a consistent and homogenous thickness. Clear short secondary foot processes of Podocytes with renal filtration slits in between were seen around the glomerular capillaries. The glomerular capillaries' endothelial cells were intimately associated with the secondary processes to constitute the filtration barrier (Figure.6). The proximal convoluted tubule lined with a tall cuboidal shape cells with euchromatic nucleus resting on uniform basal lamina. They had narrow lumen and many apical microvilli. The sections displayed many lysosomes and mitochondria. Lateral membrane interdigitation was observed (Figure.7). Distal tubule cells were cubical in shape with a euchromatic nucleus and a few short apical microvilli. The basal part had basal infoldings and mitochondria. Intact junctional complex between the cells were seen (Figure.8).

The filtration barrier of the glomerulus in diabetic group (group II) showed vacuolated capillary endothelium. The glomerular basement membrane was heterogeneous thickened. Secondary foot processes were retracted, broadened, and

shortened as a result of the podocyte effacement with obliteration of the filtration slits (Figure.9). Missing microvilli were seen in the PCT lining cells. The nucleus had an indented appearance and seemed heterochromatic. Destructed cristae caused the mitochondria to swell. Numerous vacuoles were also seen in the rarified cytoplasm (Figure.10). In DCT cells, cytoplasm had been extruded into the tubular lumen. Its nucleus was asymmetry with the expanded chromatin. Cytoplasmic vacuoles and destructed mitochondria were seen. There was separated lateral membrane (Figure.11).

Rats treated with diosmin (Group III) showed decreased thickness of glomerular homogeneous basement membrane in their renal cortex, along with obliterated capillary endothelium fenestrae. The podocytes' secondary foot processes were detected with area of effacement (Figure.12). Proximal convoluted tubule cells had regular euchromatic nuclei. Loss of microvilli in large area was observed, with cytoplasmic vacuoles and few destructed mitochondria (Figure.13). Cuboidal cells of DCT had round nucleus with extended chromatin. The luminal border showed few apical short microvilli. Cytoplasmic vacuoles DCT showed less cytoplasmic vacuolization with normal mitochondria of various sizes and shapes (Figure.14).

Gin group exhibited more improvement, where a fenestrated capillary endothelium was observed. The glomerular basement membrane thickness was apparently normal with regularly arranged, interdigitating pedicels (Figure.15). Proximal tubule cells contained euchromatic round nucleus and few cytoplasmic vacuoles with focal loss of apical microvilli (Figure.16). Cuboidal cells of distal tubules had euchromatic nucleus. Basal folding had mitochondria in between. Short microvilli lining the lumen were seen (Figure.17).

The renal cortex ultrastructure of D+G group, the glomerular filtration barrier formed of fenestrated capillary endothelium resting on regular glomerular basement. The shape of podocytes foot processes was emerged almost to control group (Figure.18). PCT, and DCT were all preserved and resembled the ultrastructure of the control group almost exactly. It was observed PCT with regular euchromatic nucleus apical microvilli and normal mitochondria. Few cytoplasmic vacuoles were detected (Figure. 19). DCT showed cuboidal cells with regular normal nucleus, mitochondria, and characteristic short microvilli lining lumen. There was an improvement in microvilli of PCT (Figure. 20).

Immunohistochemical studies

It was found that all subgroups of control group had minimal expressed desmin immunoexpression in the glomerular podocytes, but diabetic group had obvious positive expression of desmin. Desmin expression was less obvious in Dio and Gin groups. Area % of Desmin was significantly higher in Diabetic, Dio and Gin groups compared to control group. Area % of Desmin was significantly decreased in Dio, Gin and D+G groups compared to Diabetic group. Area % of Desmin revealed significantly decreased in D+G group compared to Dio group (table 3; Figure.21a-e).

The kidneys from each group are depicted in table (3) and Figures (22a-e), corresponding to immunohistochemical analyses of Nrf2. In renal tubular epithelial cells, results from control group revealed a less obvious expression of Nrf2. The renal tissues of Diabetic group had minimal Nrf2 positive regions. Area % of Nrf2 was significantly decreased in Diabetic and Dio groups compared to control group. Renal tubular epithelial cells of Dio, Gin and D+G groups also showed obvious Nrf2 expression. Area % of Nrf2 was significantly increased in Dio, Gin and D+G groups compared to Diabetic group. Area % of Nrf2 was significantly increased in D+G group compared to Dio and Gin groups.

Discussion

One of the largest healthcare problems in the world is diabetes mellitus (DM), and as the disease's prevalence rises, so do its costs. For example, according to Abhinav et al. [25], 463 million individuals globally (aged 18 to 99) were impacted by DM in 2019. The anticipated number of diabetics in Egypt was 10.9 million. By 2030, this number is expected to rise to 13 million, and by 2045, it is expected to reach 20 million [3].

Long-term hyperglycemia in diabetes mellitus results in elevated advanced glycation end products (AGEs). AGEs build up in tissue, which leads to nephropathy, target protein and lipid denaturation, and functional deterioration [26].

The goal of the current study was to examine the potential renoprotective effects of diosmin and ginger, either separately or in combination, against oxidative

stress caused by hyperglycemia in diabetic nephropathy caused by alloxan. Because alloxan can have cytotoxic effects on the pancreatic β cells, it is a commonly used medication for inducing diabetes mellitus in experimental rats [27]. The current study's alloxan-treated group exhibits the traditional diabetic nephropathy signs, namely hyperglycemia consumption. Ginger and/or diosmin therapy tend to reduce the rise in blood sugar. Our findings support the research conducted by other researchers on the potential antidiabetic benefits of natural compounds [28, 29]. Sultana et al., [30] explained that ginger can antagonize suppression of insulin release induced through serotonin receptors.

Protein metabolism's primary byproduct is urea, whereas skeletal muscle mass is represented by creatinine, a byproduct of creatinine and phosphoserine. Reduced skeletal muscle volume indicates fewer insulin target sites, which results in insulin resistance and Type 2 diabetes [31]. Generally speaking, renal impairment is indicated by elevated urea and creatinine values. In this study, diabetic rats showed considerably higher levels of kidney damage indicators, such as urea and serum creatinine, than the control group. Our findings concur with those published by Sekiou et al. [32], who discovered that these markers are markedly increased in rats with diabetes caused by alloxan. The high level of protein breakdown may be the cause of the diabetic rats' group's notable rise in those indicators of renal damage. On the other hand, we have shown that the treatment of Diosmin or/and Ginger significantly decreased blood creatinine and urea in diabetic rats, indicating a considerable reduction in protein breakdown. Our results are in good agree with earlier research [29, 33], which showed that rats given Diosmin or Ginger, respectively, saw a substantial drop in urea and creatinine.

In this work, rats given alloxan to induce diabetes showed elevation in MDA generation and a considerable reduce in SOD and CAT activity when compared to the control group. This is in line with previous studies [32, 34], which showed that after being exposed to alloxan, MDA levels rose while SOD and CAT levels dropped. Intracellular auto-oxidation of glucose to glycol is brought on by AGEs. More free radicals are produced when the reactive products combine with the amino groups of extracellular and intracellular proteins to create AGEs. Lipid peroxidation and MDA formation are the results of increased oxidative stress [35].

Conversely, In groups treated with diosmin or/and ginger, there was a considerable decrease in MDA levels accompanied by significantly higher SOD and catalase activity, suggesting that the antioxidant system has been activated to counterbalance the excess ROS generated. These results concur with those of previous research that also revealed treatment with diosmin or/ and ginger significantly increase SOD and catalase activity and significantly decrease in MDA level demonstrating its potent antioxidant action and lowers cell death by binding with free radicals [8, 36].

Under hematoxylin and eosin staining, the renal cortex sections of the alloxan-induced diabetic group in this study had dilated Bowman space and glomerular abnormalities. Detached cells were present into the lumen tubules. The results that were reported earlier agreed with these findings [37]. Electron analyses of the renal cortex support these conclusions. In addition to podocyte effacement, the glomerular basement membrane was unevenly thickened. Abrupt loss of apical microvilli was seen in PCT cells. Cytoplasmic vacuolations, enlarged mitochondria, and pyknotic nuclei were all seen. The intracellular space between the cells exhibiting cytoplasmic vacuolations increased in DCT cells. These findings are agree with earlier research [38, 39], who noted kidney alterations in diabetes caused by streptozotocin. This might be because excessive extracellular matrix formation and mechanical stretching are brought on by hyperglycemia's induction of hyperfiltration and hyperperfusion [40].

In the present study, Gin group showed improvement of diabetic-induced degenerative changes after administration of ginger. Ultrastructurally, a regular thickness of basement membrane and attenuation of effacement with few vacuolization in PT were seen. Similar results were reported in previous studies [13, 41, 42]. This could be attributed to the hypoglycemic effect of ginger. Ginger was shown to reduce inflammatory markers in diabetic individuals [43]. In addition, it can improve the oxidative stress and has antiapoptotic role [13, 44].

Rats given a combination of diosmin and ginger in our investigation showed a more noticeable improvement in diabetic-induced renal degenerative disease. This study aligns with the goal of creating a cosmeceutical preparation that carries Diosmin in conjunction with various essential oils, like Zingiber officinale (ginger oil), to function as both preventive and curative dermal novel preparations, aimed at battling

harmful environmental factors that impact the skin. The generated lipoid colloidal carriers (LCCs) were evaluated, and the addition of the mentioned ginger oil was found to improve the Diosmin action in both in-vitro and in-vivo investigations [45].

Desmin function is to raise the mechanical resistance of the cells, when its expression increases in podocytes it represents an indicator of morphological changes of these podocytes in reaction to injury [46]. Immunohistochemical staining for Desmin of diabetic group revealed, intense positive immune reaction of glomerular podocytes as compared to the control group. Moreover, moderate immune reaction of glomerular podocytes was observed in groups treated with diosmin or ginger. Administration of diosmin and ginger in diabetic rats had weak reaction similar to control group. Previous studies suggested that diosmin and ginger have a strong antioxidant, anti-inflammatory, antifibrotic, immunomodulating and antiapoptotic properties [8, 36].

To further explain the route, the immunohistochemistry of Nrf2 was examined. In renal tubular epithelial cells, Diabetic group had weak Nrf2 positive regions. These findings were consistent with Abdul-Hamid et al. [38] and Chen et al. [47] who found that Streptozotocin-induced diabetes caused significant decreases in Nrf2 level. Renal tubular epithelial cells of groups treated with Diosmin and Ginger also showed considerable Nrf2 expression. Compared to other groups, D+G group had higher intense of positive regions for Nrf2 which showed a protective effect of diosmin and ginger against diabetic-induced nephropathy. It was shown in an animal study that Nrf2 plays a critical role in reducing the kidney damage caused by streptozotocin. This is demonstrated by the fact that Nrf2-/ mice produce more ROS than Nrf2+/ mice, and they also have more kidney damage and oxidative DNA damage [48]. Another study found that the diabetic group's spleen had much less Nrf2 expression than the control group's because hyperglycemia, which causes diabetes, stimulates Keap1 (Kelch like associated protein-1) malfunction.Another study found that the diabetic group's spleen had much less Nrf2 expression than the control group's because hyperglycemia, which causes diabetes, stimulates Keap1 (Kelch like associated protein-1) malfunction [49].

Conclusions

From this study, we concluded that treatment with diosmin showed minimal improvement in the changes in glomerular structure, PCT, and DCT, compared with diabetic rats treated with ginger. Considering the efficacy of combination therapy of diosmin and ginger, the current results showed a significant ameliorative effect on all histopathological features and biochemical markers on the kidneys of diabetic rats.

References

1. Lucchesi, A. N., Freitas, N. T. D., Cassettari, L. L., Marques, S. F. G., & Spadella, C. T. (2013). Diabetes mellitus triggers oxidative stress in the liver of alloxan-treated rats: a mechanism for diabetic chronic liver disease. Acta Cirurgica Brasileira, 28, 502-508.
   DOI: 10.1590/s0102-86502013000700005
2. Singh, B., Kumar, A., Singh, H., Kaur, S., Kaur, S., Buttar, H. S., ... & Singh, B. (2020). Zingerone produces antidiabetic effects and attenuates diabetic nephropathy by reducing oxidative stress and overexpression of NF-κB, TNF-α, and COX-2 proteins in rats. Journal of Functional Foods, 74, 104199.
   https://doi.org/10.1016/j.jff.2020.104199.
3. Saeedi, P., Petersohn, I., Salpea, P., Malanda, B., Karuranga, S., Unwin, N., ... & IDF Diabetes Atlas Committee. (2019). Global and regional diabetes prevalence estimates for 2019 and projections for 2030 and 2045: Results from the International Diabetes Federation Diabetes Atlas. Diabetes research and clinical practice, 157, 107843.
   DOI: 10.1016/j.diabres.2019.107843.
4. Gonzalez-Gonzalez, M., Yerena-Prieto, B. J., Carrera, C., Vázquez-Espinosa, M., González-de-Peredo, A. V., García-Alvarado, M. Á., ... & Barbero, G. F. (2023). Optimization of an Ultrasound-Assisted Extraction Method for the Extraction of Gingerols and Shogaols from Ginger (Zingiber officinale). Agronomy, 13(7), 1787.
   DOI: 10.3390/agronomy12020261
5. Mahomoodally, M. F., Aumeeruddy, M. Z., Rengasamy, K. R., Roshan, S., Hammad, S., Pandohee, J., ... & Zengin, G. (2021, February). Ginger and its active compounds in cancer therapy: From folk uses to nano-therapeutic

applications. In Seminars in cancer biology (Vol. 69, pp. 140-149). Academic Press.
DOI: 10.1016/j.semcancer.2019.08.009.

6. AL Badawi, M. H., Waly, N. E., Eid, M. M., & Soliman, N. A. (2022). Histopathological impact of Ginger loaded nanoparticle versus ginger extract as a novel therapy of experimentally induced acute ulcerative colitis. Egyptian Journal of Histology, 45(2), 442-456.
DOI: 10.21608/ejh.2021.68124.1448
7. Boarescu, I., Pop, R. M., Boarescu, P. M., Bocșan, I. C., Gheban, D., Bulboacă, A. E., ... & Bolboacă, S. D. (2023). Ginger (Zingiber officinale) root capsules enhance analgesic and antioxidant efficacy of diclofenac sodium in experimental acute inflammation. *Antioxidants*, *12*(3), 745.
DOI: 10.3390/antiox12030745.
8. Huwait, E., & Mobashir, M. (2022). Potential and therapeutic roles of diosmin in human diseases. *Biomedicines*, *10*(5), 1076.
DOI: 10.3390/biomedicines10051076.
9. Ağır, M. S., & Eraslan, G. (2019). The effect of diosmin against liver damage caused by cadmium in rats. *Journal of food biochemistry*, *43*(9), e12966.
https://doi.org/10.1111/jfbc.12966.
10. Liu, X., Zhang, X., Zhang, J., Kang, N., Zhang, N., Wang, H., ... & Wang, X. (2014). Diosmin protects against cerebral ischemia/reperfusion injury through activating JAK2/STAT3 signal pathway in mice. *Neuroscience*, *268*, 318-327.
DOI: 10.1016/j.neuroscience.2014.03.032.
11. Mirshekar, M. A., Fanaei, H., Keikhaei, F., & Javan, F. S. (2017). Diosmin improved cognitive deficit and amplified brain electrical activity in the rat model of traumatic brain injury. *Biomedicine & Pharmacotherapy*, *93*, 1220-1229.
DOI: 10.1016/j.biopha.2017.07.014.
12. Anwer, T., Alshahrani, S., Somaili, A. M., Khubrani, A. H., Ahmed, R. A., Jali, A. M., ... & Alam, M. F. (2023). Nephroprotective effect of diosmin against cisplatin-induced kidney damage by modulating IL-1β, IL-6, TNFα and renal oxidative damage. Molecules, 28(3), 1302.
DOI: 10.3390/molecules28031302

13. Elsayed, H. M., Abdel-Aziz, H. O., Ahmed, G. M., Adly, M. A., & Mohammed, S. A. (2023). The Possible Ameliorative Effect of Echinacea, Ginger, and Their Combination on Experimentally Induced Diabetic Nephropathy in a Rat Model: Histological and Immunohistochemical Study. *Journal of Microscopy and Ultrastructure*.
DOI:10.4103/jmau.jmau_62_22.
14. Hamadjida, A., Mbomo, R. E. A., Minko, S. E., Ntchapda, F., Mingoas, J. P. K., & Nnanga, N. (2024). Antioxidant and anti-inflammatory effects of Boswellia dalzielii and Hibiscus sabdariffa extracts in alloxan-induced diabetic rats. Metabolism Open, 21, 100278.
DOI: 10.1016/j.metop.2024.100278.
15. Fawcett, J., & Scott, J. (1960). A rapid and precise method for the determination of urea. *Journal of clinical pathology*, *13*(2), 156-159.
DOI: 10.1136/jcp.13.2.156.
16. MZ, J. (1886). Niederschlag welchen pikrinsaure in normalen Harn erzeugt and Uber eine neue Reakion des Kreatinis. *Z Phisiol Chem*, *10*, 391.
https://doi.org/10.1515/bchm1.1886.10.5.391.
17. Preuss, H. G., Jarrell, S. T., Scheckenbach, R., Lieberman, S., & Anderson, R. A. (1998). Comparative effects of chromium, vanadium and Gymnema sylvestre on sugar-induced blood pressure elevations in SHR. Journal of the American College of Nutrition, 17(2), 116-123.
DOI: 10.1080/07315724.1998.10718736.
18. Marklund, S., & Marklund, G. (1974). Involvement of the superoxide anion radical in the autoxidation of pyrogallol and a convenient assay for superoxide dismutase. *European journal of biochemistry*, *47*(3), 469-474.
DOI: 10.1111/j.1432-1033.1974.tb03714.x.
19. Cohen, G., Dembiec, D., & Marcus, J. (1970). Measurement of catalase activity in tissue extracts. *Analytical biochemistry*, *34*(1), 30-38.
DOI: 10.1016/0003-2697(70)90083-7.
20. Bancroft, J. D., & Layton, C. (2012). Connective and mesenchymal tissues with their stains. *Bancroft's Theory and practice of histological techniques*, 187-214.
https://doi.org/10.1016/C2015-0-00143-5.

21. Jakkson, P., & Blqthe, D. (2013). Immunohistochemical performances [chapter 8]. *Theory and run-through of histological techniques. 7th ed. Philadelphia: Churchill Livingstone of Elsevier*, 267-376. https://doi.org/10.1016/C2015-0-00143-5

22. Wiggins, J. E., Goyal, M., Sanden, S. K., Wharram, B. L., Shedden, K. A., Misek, D. E., ... & Wiggins, R. C. (2005). Podocyte hypertrophy,"adaptation," and "decompensation" associated with glomerular enlargement and glomerulosclerosis in the aging rat: prevention by calorie restriction. Journal of the American Society of Nephrology, 16(10), 2953-2966. DOI: 10.1681/ASN.2005050488

23. Zhao, W., Huang, X., Zhang, L., Yang, X., Wang, L., Chen, Y., ... & Wu, G. (2016). Penehyclidine hydrochloride pretreatment ameliorates rhabdomyolysis-induced AKI by activating the Nrf2/HO-1 pathway and allevi-ating endoplasmic reticulum stress in rats. PLoS One, 11(3), e0151158. https://doi.org/10.1371/journal.pone.0151158

24. Hayaty, M. A. (2000). Chemical fixation [chapter 2]. *Principles and techniques of biological applications. 4th ed. UK: Cambridge University Press*, 7-99. DOI:10.1006/anbo.2001.1367.

25. Abhinav, R. P., Williams, J., Livingston, P., Anjana, R. M., & Mohan, V. (2020). Burden of diabetes and oral cancer in India. *Journal of Diabetes and its Complications*, *34*(11), 107670. https://doi.org/10.1016/j.jdiacomp.2020.107670

26. Wu, T., Ding, L., Andoh, V., Zhang, J., & Chen, L. (2023). The mechanism of hyperglycemia-induced renal cell injury in diabetic nephropathy disease: an update. *Life*, *13*(2), 539. DOI: 10.3390/life13020539

27. Kanthlal, S. K., Kumar, B. A., Joseph, J., Aravind, R., & Frank, P. R. (2014). Amelioration of oxidative stress by Tabernamontana divaricata on alloxan-induced diabetic rats. *Ancient Science of Life*, *33*(4), 222-228. DOI: 10.4103/0257-7941.147429.

28. Singh, B., Kumar, A., Singh, H., Kaur, S., Kaur, S., Buttar, H. S., ... & Singh, B. (2020). Zingerone produces antidiabetic effects and attenuates diabetic

nephropathy by reducing oxidative stress and overexpression of NF-κB, TNF-α, and COX-2 proteins in rats. *Journal of Functional Foods*, *74*, 104199. https://doi.org/10.1016/j.jff.2020.104199

29. Ahmed, S., Mundhe, N., Borgohain, M., Chowdhury, L., Kwatra, M., Bolshette, N., ... & Lahkar, M. (2016). Diosmin modulates the NF-kB signal transduction pathways and downregulation of various oxidative stress markers in alloxan-induced diabetic nephropathy. *Inflammation*, *39*, 1783-1797. DOI: 10.1007/s10753-016-0413-4.
30. Sultana, S., Khan, M. I., Rahman, H., Nurunnabi, A. S. M., & Afroz, R. D. (2014). Effects of ginger juice on blood glucose in alloxan induced diabetes mellitus in rats. *Journal of Dhaka Medical College*, *23*(1), 14-17. DOI:10.1007/s11356-020-11944-0
31. Palsamy, P., & Subramanian, S. (2011). Resveratrol protects diabetic kidney by attenuating hyperglycemia-mediated oxidative stress and renal inflammatory cytokines via Nrf2–Keap1 signaling. *Biochimica et Biophysica Acta (BBA)-Molecular Basis of Disease*, *1812*(7), 719-731. DOI: 10.1016/j.bbadis.2011.03.008.
32. Sekiou, O., Boumendjel, M., Taibi, F., Tichati, L., Boumendjel, A., & Messarah, M. (2021). Nephroprotective effect of Artemisia herba alba aqueous extract in alloxan-induced diabetic rats. *Journal of traditional and complementary medicine*, *11*(1), 53-61. DOI: 10.1016/j.jtcme.2020.01.001.
33. Abd Elwahab, A. H., & Ali, F. I. (2015). Mitigation of alloxane-induced renal damage by Zingiber officinale (ginger) root in rats: an impact on oxidative stress, inflammatory cytokines and tissue damage. *Al-azhar Assiut Medical Journal*, *13*(1), 158.
34. Das, J., & Sil, P. C. (2012). Taurine ameliorates alloxan-induced diabetic renal injury, oxidative stress-related signaling pathways and apoptosis in rats. *Amino acids*, *43*, 1509-1523. https://doi.org/10.1007/s00726-012-1225-y
35. Pal, P. B., Sinha, K., & Sil, P. C. (2014). Mangiferin attenuates diabetic nephropathy by inhibiting oxidative stress mediated signaling cascade, TNFα related and mitochondrial dependent apoptotic pathways in streptozotocin-induced diabetic rats. *PloS one*, *9*(9), e107220.

https://doi.org/10.1371/journal.pone.0107220.

36. Al Hroob, A. M., Abukhalil, M. H., Alghonmeen, R. D., & Mahmoud, A. M. (2018). Ginger alleviates hyperglycemia-induced oxidative stress, inflammation and apoptosis and protects rats against diabetic nephropathy. *Biomedicine & Pharmacotherapy*, *106*, 381-389. https://doi.org/10.1016/j.biopha.2018.06.148.
37. Pansare, K., Upasani, C., Upangalwar, A., Sonawane, G., & Patil, C. (2021). Streptozotocin and alloxan induced diabetic nephropathy: protective role of natural products. *Journal of the Maharaja Sayajirao University of Baroda ISSN*, *25*, 0422.
38. Abdul-Hamid, M., Galaly, S. R., Mohamed, H. M., Mostafa, F., & Abdel-Moneim, A. (2023). Polydatin nanoparticles attenuate oxidative stress and histopathological changes in streptozotocin model of diabetic nephropathy: targeting Nrf2/HO-1/NF-κβ signaling pathways. Beni-Suef University Journal of Basic and Applied Sciences, 12(1), 99. https://doi.org/10.1186/s43088-023-00441-1
39. Ebrahim, N., Ahmed, I. A., Hussien, N. I., Dessouky, A. A., Farid, A. S., Elshazly, A. M., ... & Sabry, D. (2018). Mesenchymal stem cell-derived exosomes ameliorated diabetic nephropathy by autophagy induction through the mTOR signaling pathway. *Cells*, *7*(12), 226. https://doi.org/10.3390/cells7120226.
40. Uil, M., Scantlebery, A. M., Butter, L. M., Larsen, P. W., de Boer, O. J., Leemans, J. C., ... & Roelofs, J. J. (2018). Combining streptozotocin and unilateral nephrectomy is an effective method for inducing experimental diabetic nephropathy in the 'resistant'C57Bl/6J mouse strain. *Scientific Reports*, *8*(1), 5542. https://doi.org/10.1038/s41598-018-23839-9
41. Payami, S. A., Babaahmadi-Rezaei, H., Ghaffari, M. A., Mansouri, E., & Mohammadzadeh, G. (2019). Hydroalcoholic Extract of Zingiber officinale Improves STZ-Induced Diabetic Nephropathy in Rats by Reduction of NF-κB Activation. *Jundishapur Journal of Natural Pharmaceutical Products*, *14*(2):e55063. https://doi.org/10.5812/jjnpp.55063.

42. Al-Qudah, M., Al-Ramamneh, E. A. D., Haddad, M. A., & Al-Abbadi, A. (2018). The histological effect of aqueous ginger extract on kidneys and lungs of diabetic rats. *International Journal of Biology*, *10*(4), 23-28. https://doi.org/10.5539/ijb.v10n4p23.

43. Arablou, T., Aryaeian, N., Valizadeh, M., Sharifi, F., Hosseini, A., & Djalali, M. (2014). The effect of ginger consumption on glycemic status, lipid profile and some inflammatory markers in patients with type 2 diabetes mellitus. *International journal of food sciences and nutrition*, *65*(4), 515-520. https://doi.org/10.3109/09637486.2014.880671.

44. Moawad, A. A., & Abo Baker, S. H. (2020). Histological Assessment of ginger (Zingiber officinale) extract on tongue dorsal surface in diabetic rats. *Egyptian Dental Journal*, *66*(2-April (Oral Medicine, X-Ray, Oral Biology & Oral Pathology)), 991-996. DOI: 10.21608/EDJ.2020.25445.1064

45. Kamel, R., Abbas, H., & Fayez, A. (2017). Diosmin/essential oil combination for dermal photo-protection using a lipoid colloidal carrier. *Journal of photochemistry and photobiology B: biology*, *170*, 49-57. https://doi.org/10.1016/j.jphotobiol.2017.03.019.

46. Funk, J., Ott, V., Herrmann, A., Rapp, W., Raab, S., Riboulet, W., ... & Jacobsen, B. (2016). Semiautomated quantitative image analysis of glomerular immunohistochemistry markers desmin, vimentin, podocin, synaptopodin and WT-1 in acute and chronic rat kidney disease models. *Histochemistry and cell biology*, *145*, 315-326. https://doi.org/10.1007/s00418-015-1391-6

47. Chen, H. W., Yang, M. Y., Hung, T. W., Chang, Y. C., & Wang, C. J. (2019). Nelumbo nucifera leaves extract attenuate the pathological progression of diabetic nephropathy in high-fat diet-fed and streptozotocin-induced diabetic rats. *journal of food and drug analysis*, *27*(3), 736-748. https://doi.org/10.1016/j.jfda.2018.12.009

48. Jiang, T., Huang, Z., Lin, Y., Zhang, Z., Fang, D., & Zhang, D. D. (2010). The protective role of Nrf2 in streptozotocin-induced diabetic nephropathy. *Diabetes*, *59*(4), 850-860. https://doi.org/10.2337/db09-1342.

49. Mohamed, E. M., Reda, A. M., & Elnegris, H. M. (2021). Role of L-carnitine treated mesenchymal stem cells on histological changes in spleen of experimentally induced diabetic rats and the active role of Nrf2 signaling. Egyptian Journal of Histology, 44(3), 630-642.
DOI: 10.21608/ejh.2020.34159.1323

الملخص العربى

إمكانات الحماية الكلوية للزنجبيل والديوسمين ومزيجهما في اعتلال الكلية السكري المستحث في نموذج الفئران: الملاحظات المجهرية الضوئية والإلكترونية

مقدمة

ارتفاع السكر في الدم هو مرض مزمن يرتبط بمرض السكري. وقد وجد أن المرضى الذين يعانون من مرض السكري لديهم العديد من التغييرات في وظائف الكلى. كان الهدف من هذه الدراسة هو تقييم الفوائد المحتملة للديوسمين والزنجبيل ، إما بشكل منفصل أو كلاهما ، لاعتلال الكلية السكري الذي تم إنتاجه تجريبيا.

المواد والطرق المستخدمة

المجموعة الأولى ، استخدمت عشرة فئران للمجموعة الضابطة. أعطيت جميع الفئران (باستثناء المجموعة الضابطة) جرعة واحدة داخل الصفاق من ألوكسان (150 ملغم / كغم من وزن الجسم) للحث على مرض السكري من النوع الثانى. تألفت المجموعة الثانية من عشرة فئران مصابة بالسكري. تلقت عشرة فئران مصابة بالسكري 100 مغ/كغ من الديوسمين عن طريق الفم لمدة ستة أسابيع كجزء من المجموعة الثالثة. عشرة فئران مصابة بالسكري. تلقى جزء من المجموعة الرابعة 400 ملغم / كغم من الزنجبيل عن طريق الفم لمدة ستة أسابيع. تلقت عشرة فئران مصابة بالسكري في المجموعة الخامسة علاجا عن طريق الفم لمدة ستة أسابيع بالزنجبيل (400 مغ/كغ) والديوسمين (100 مغ/كغ). تم التضحية بالفئران بعد الأسابيع الستة ، وتم أخذ عينات من أنسجة الكلى والدم لإجراء العديد من التحليلات الكيميائية الحيوية. كما تم تحضير النسيج الكلوى للفحص تحت المجهر الضوئي والإلكتروني. تم استخدام علامات desmin و Nrf2 المناعية الكيميائية لإجراء دراسات إحصائية ومورفومترية.

النتائج:

يؤدي علاج الديوسمين بالإضافة إلى الزنجبيل إلى انخفاض كبير في نسبة الجلوكوز في الدم واليوريا والكرياتينين على عكس الفئران المصابة بداء السكري. بعد ستة أسابيع ، كان هناك انتعاش ملحوظ في مستويات (MDA) ، الكاتلاز (CAT) وديسموتاز الفائق (SOD). أثبت التحليل النسيجي المرضي أن

المجموعة الخامسة تستعيد بالمثل البنية الطبيعية للأنسجة الكلوية. عند مقارنتها بمجموعة مرضى السكري ، كانت النسبة المئوية لمساحة Desmin في المجموعة الخامسة أقل بكثير ، في حين زادت مساحتها فى Nrf2.

الخلاصة:

أظهر علاج الزنجبيل بمفرده أو بالاشتراك مع الديوسمين تحسنا أكثر وضوحا في اعتلال الكلية السكري.

Figure 1: A photomicrograph of kidney section in control group, illustrating the glomerular capillaries (c) ad Bowman's capsule (arrow) with normal Bowman's space (star). PCT (green head arrow) with luminal brush border (curved arrow) and DCT (yellow head arrow) can be seen. **(H and E X400)**

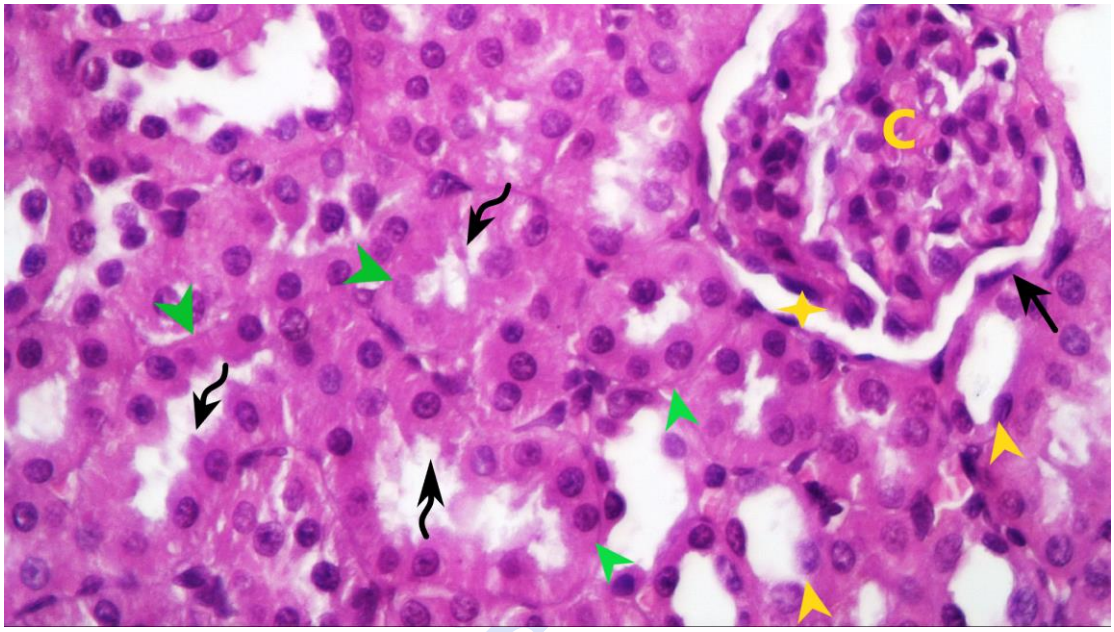

Figure 2: A photomicrograph of kidney section in Diabetic group, illustrating the shrinkage glomerular capillaries (c) with widening of urinary space (star). Loss of brush border of proximal tubules (green head arrow) can be noticed. The renal tubular epithelial cells show vacuolations (cross). Some of detached cells present into the lumen tubules (curved arrow). **(H and E X400)**

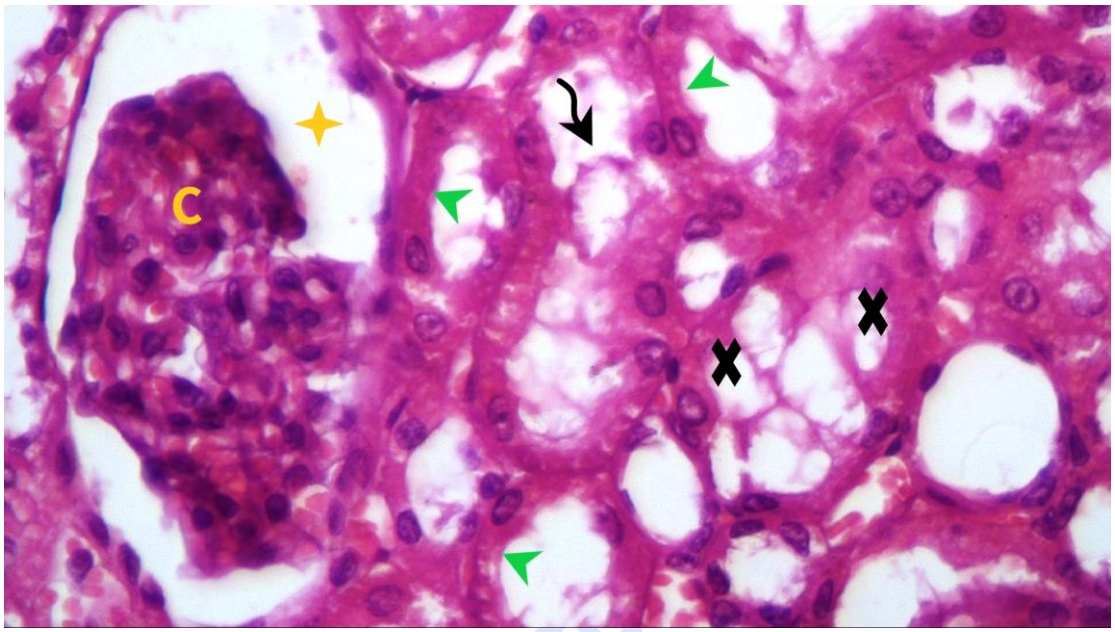

Figure 3: A photomicrograph of kidney section in Dio group, illustrating glomerulus (c) with normal urinary space (star). Some cells of proximal tubules (green head arrow) appear slightly normal while the other shows vacuolated cytoplasm (cross) with darkly stained nuclei (curved arrow). **(H and E X400)**

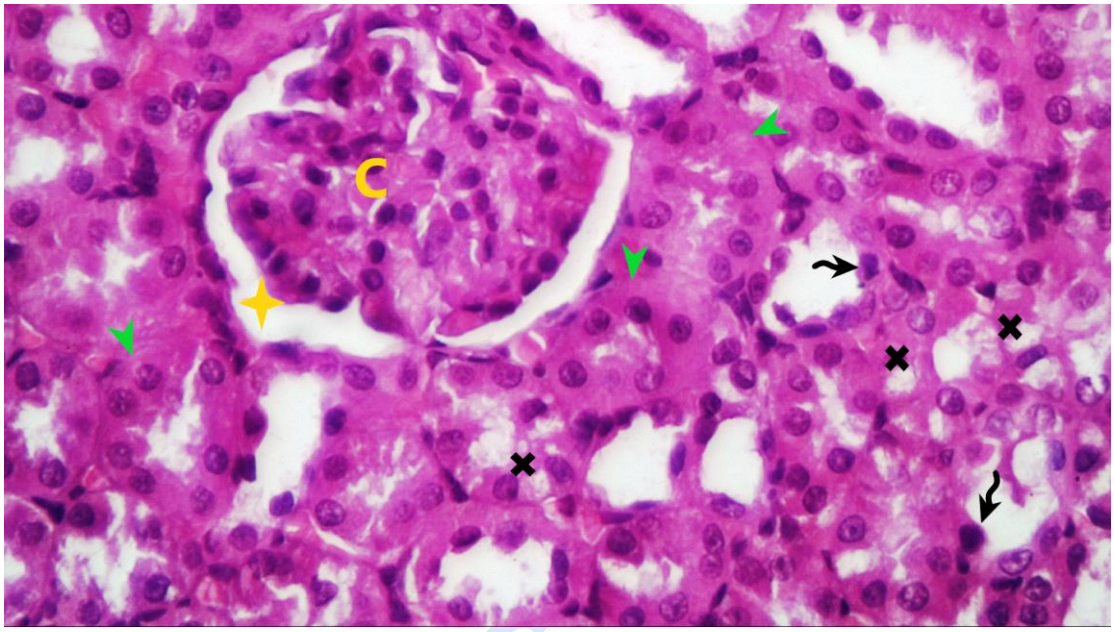

Figure 4: A photomicrograph of kidney section in Gin group, illustrating glomerulus (c) with normal urinary space (star). Proximal convoluted tubules (green head arrow) have apical brush border. Few vacuolated cells (cross) in convoluted tubules can be observed. Congested peritubular blood vessels (v) are present. **(H and E x400)**

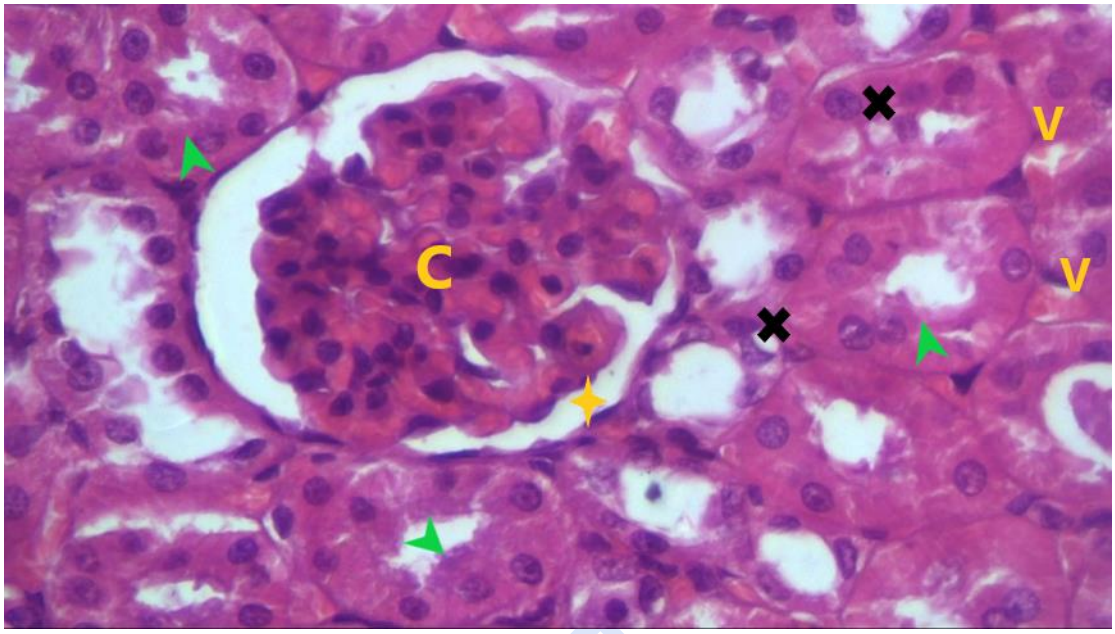

Figure 5: A photomicrograph of kidney section in D+G group, illustrating apparently normal of the glomerular capillaries (c) and urinary space (star). Notice near normal proximal (green head arrow) and distal convoluted tubules (yellow head arrow). Congested peritubular blood vessels (v) are present**. (H and E x400)**

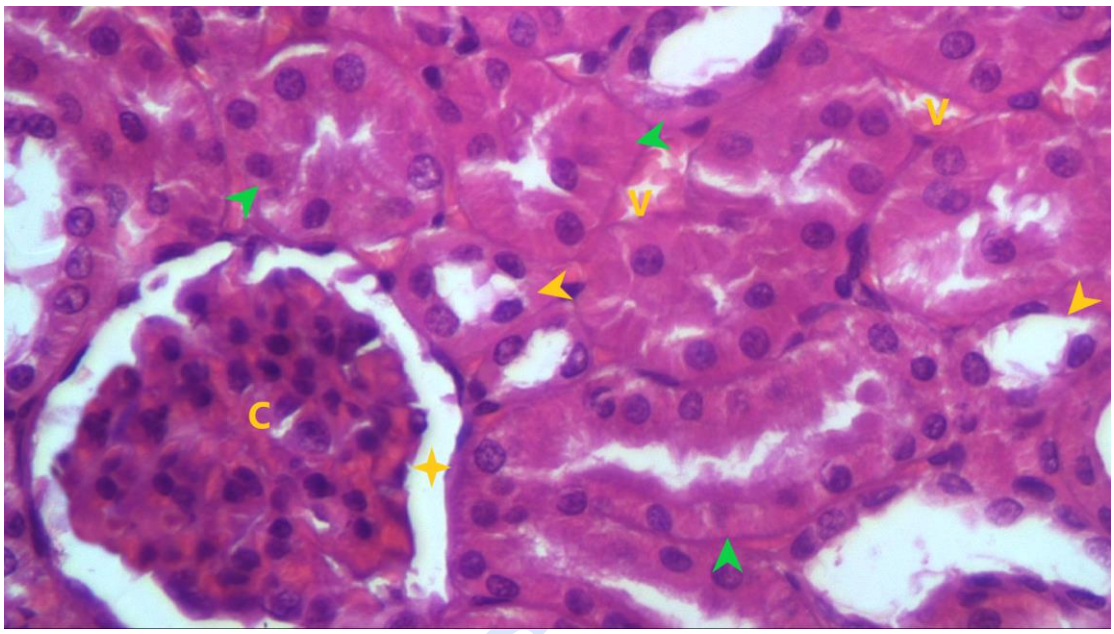

Figure 6: Transmission electron micrograph of kidney section from control group, illustrating filtration barrier of the glomerulus consists of a fenestrated capillary endothelium (curved arrow). The basement membrane (arrow) is a regular, homogenous. The secondary foot processes of the pododcytes (yellow head arrow) with filtration slit (green head arrow) in between. **(electron microscopy, x 6000)**

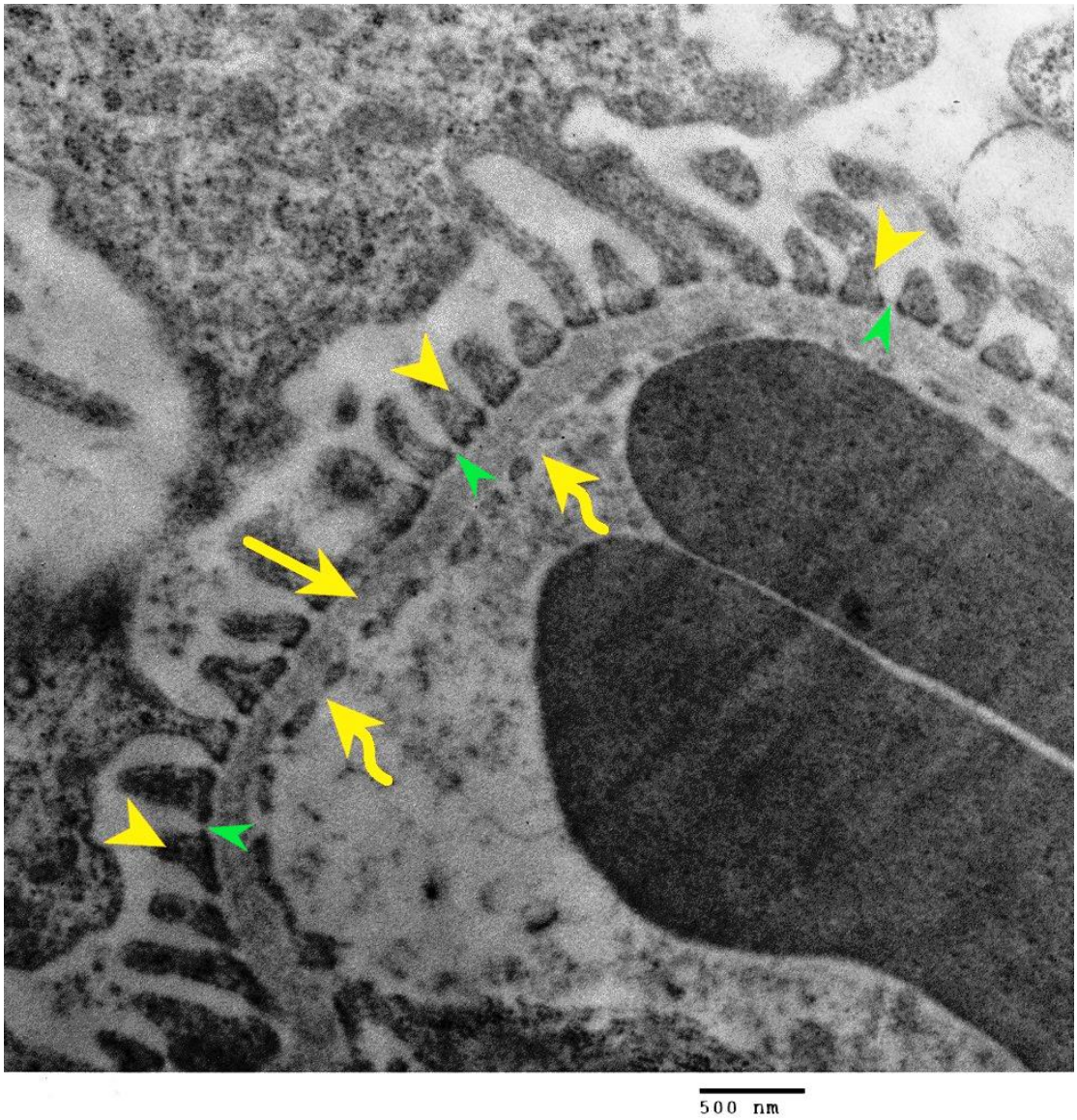

Figure 7: Transmission electron micrograph of PCT in kidney section of control group, illustrating tall cuboidal cells lying down on slim uniform basal lamina (curved arrow). Round euchromatic nucleus (N) is observed. Luminal border shows long tightly packed microvilli (arrow). Elongated mitochondria (m), lysosomes (L) and lipid droplets (i) can be observed. Notice intact junctional complex between the cells (head arrow). **(electron microscopy, x 1500)**

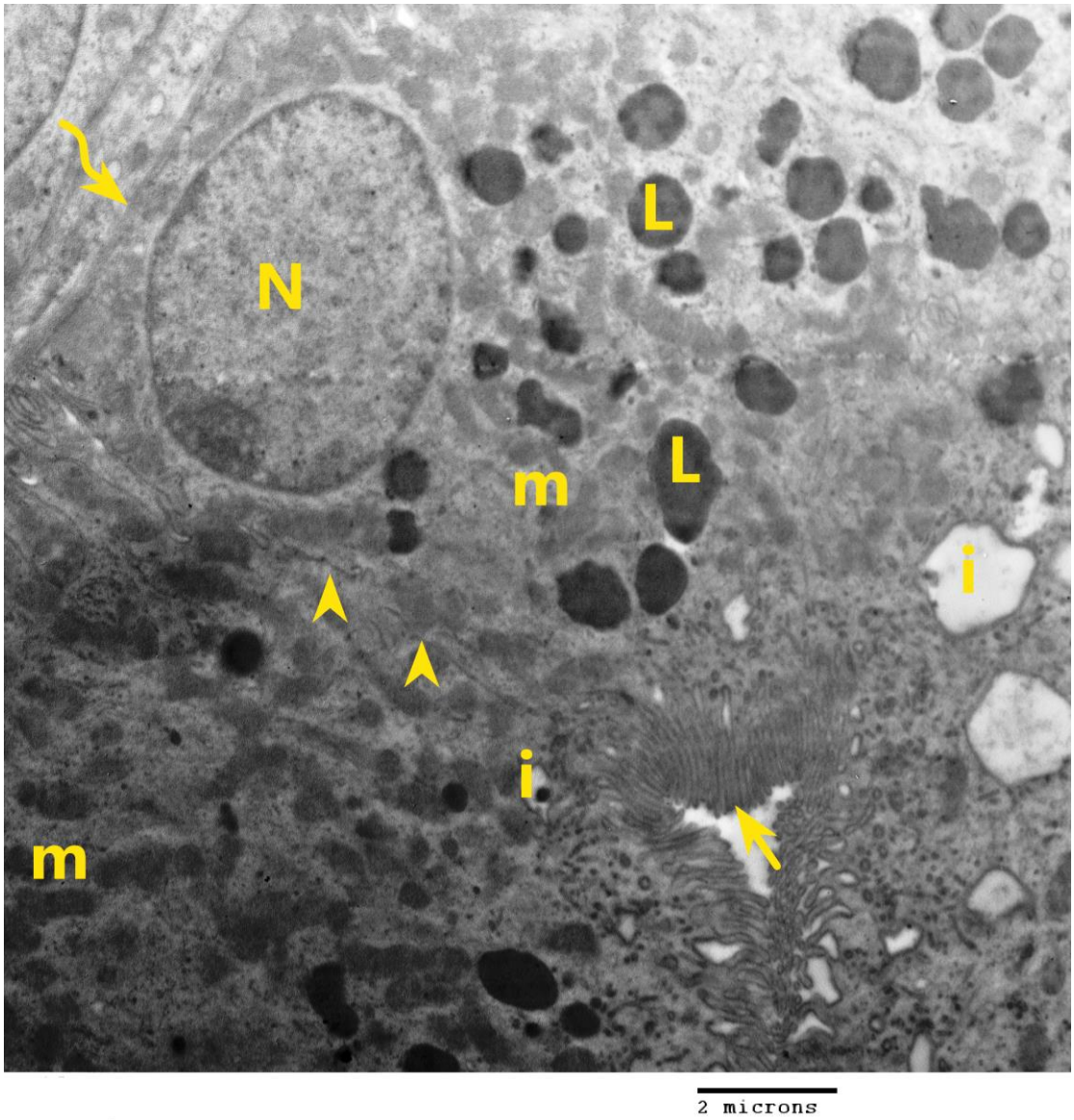

Figure 8: Transmission electron micrograph of DCT of control group illustrating cubical cells lying down on thin basal lamina (curved arrow) with euchromatic nucleus (N). The cells have apical short microvilli (arrow). There are basal infoldings with their mitochondria (m). Notice, intact junctional complex between the cells (head arrow). **(electron microscopy, x 1500)**

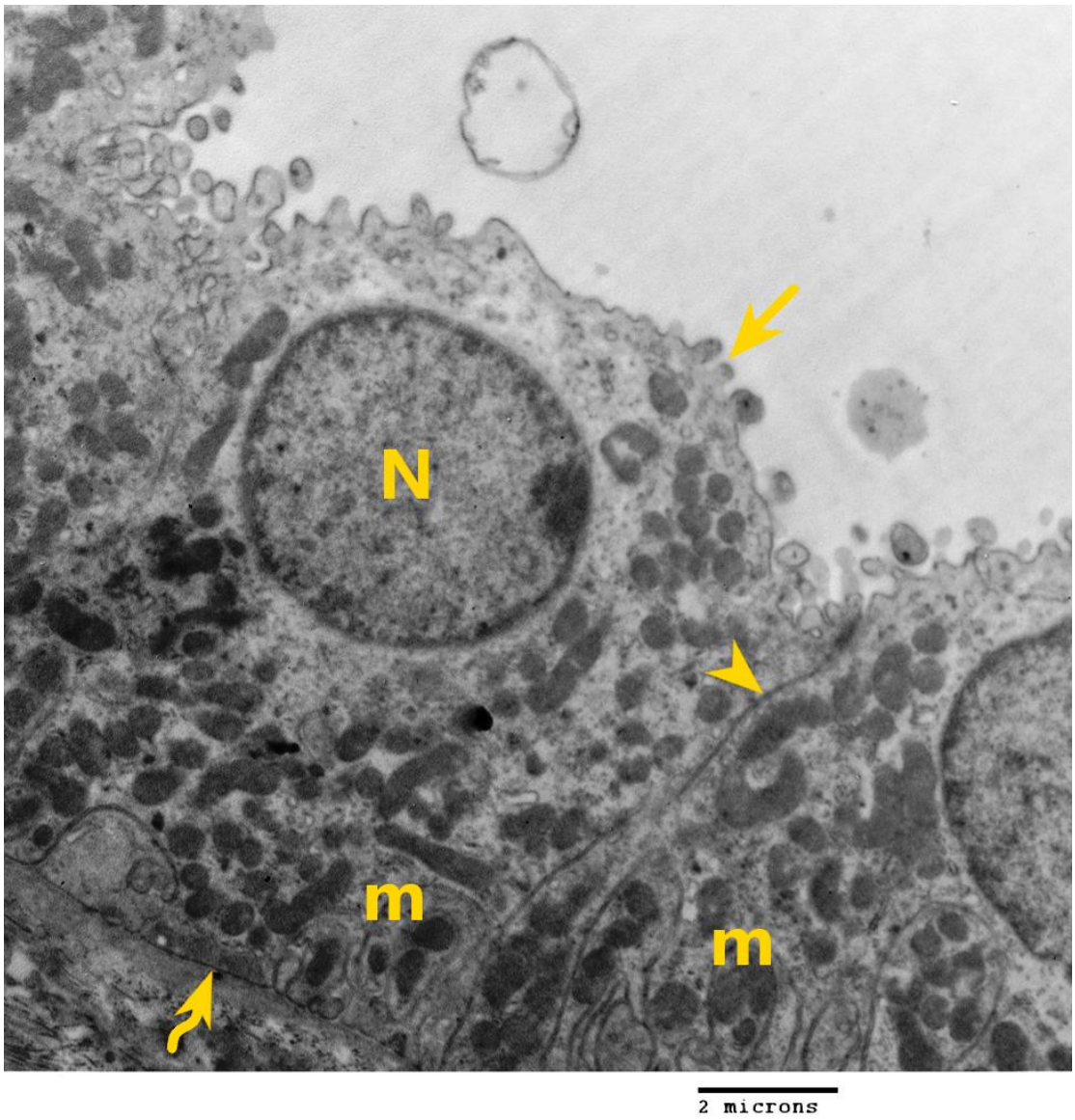

Figure 9: Transmission electron micrograph of kidney section from Diabetic group, illustrating the filtration barrier of the glomerulus with vacuolated capillary endothelium (curved arrow). The basement membrane (arrow) is thickened and heterogenous. Obliteration of the filtration slits (green head arrow) can be observed with disarrangement the secondary foot processes of the pododcytes (yellow head arrow). **(electron microscopy, x 6000)**

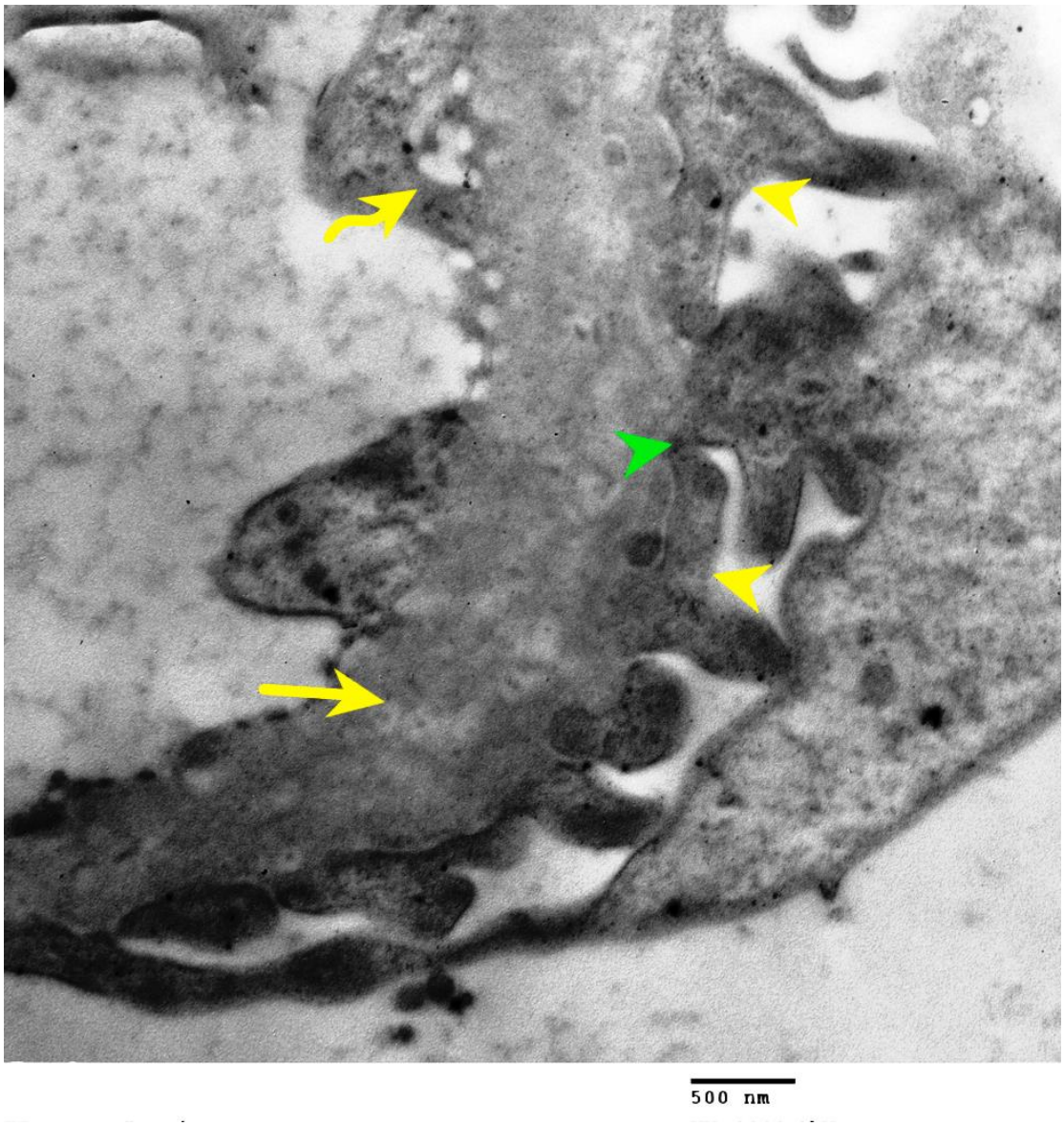

Figure 10: Transmission electron micrograph of PCT from kidney section of Diabetic group, illustrating lining cell resting on destructed irregular basal lamina (curved arrow) with dark pyknotic nucleus (N). Damaged microvilli (arrow) can be seen in the denuded luminal border. Notice rarified vacuolated cytoplasm (star) and destructed mitochondria (head arrow). **(electron microscopy, x 1500)**

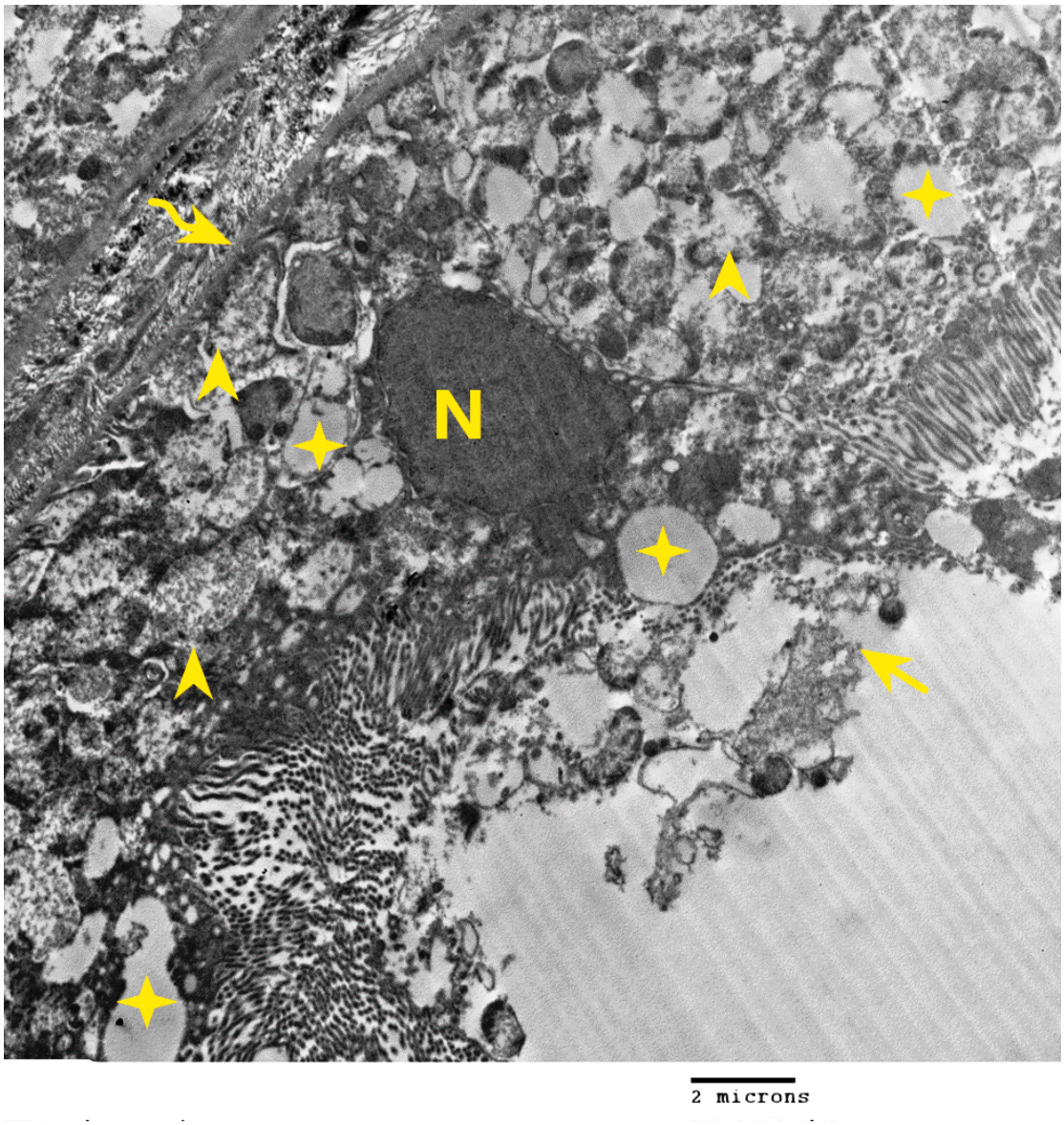

Figure 11: Transmission electron micrograph of DCT from Diabetic group, illustrating cuboidal cells of DCT resting on destructed basal lamina (curved arrow). It is noticed that the nucleus (N) is irregular with abnormal distributed chromatin. Extruded cytoplasm bursts the apical portion and enters the tubular lumen (arrow). Vacuolated cytoplasm (star) and destructed mitochondria (m) are seen. Notice separated lateral membrane (head arrow). **(electron microscopy, x 1500)**

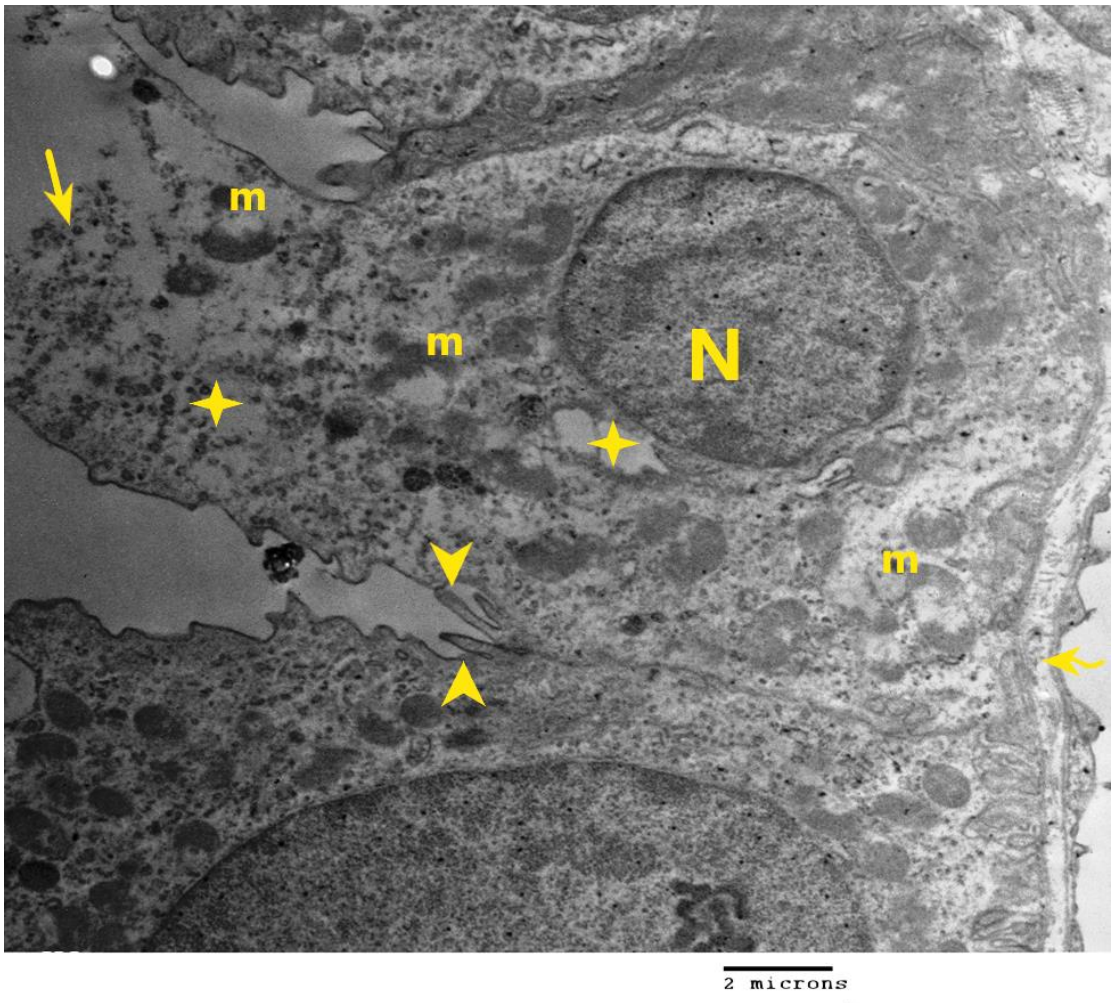

Figure 12: Transmission electron micrograph of kidney section from Dio group, illustrating obliterated fenestrae of capillary endothelium (curved arrow) with less thickening in homogenous glomerular basement membrane (arrow). The secondary foot processes of podocytes show area of effacement (yellow head arrow). Also, filtration slit can be seen (green head arrow). **(electron microscopy, x 6000)**

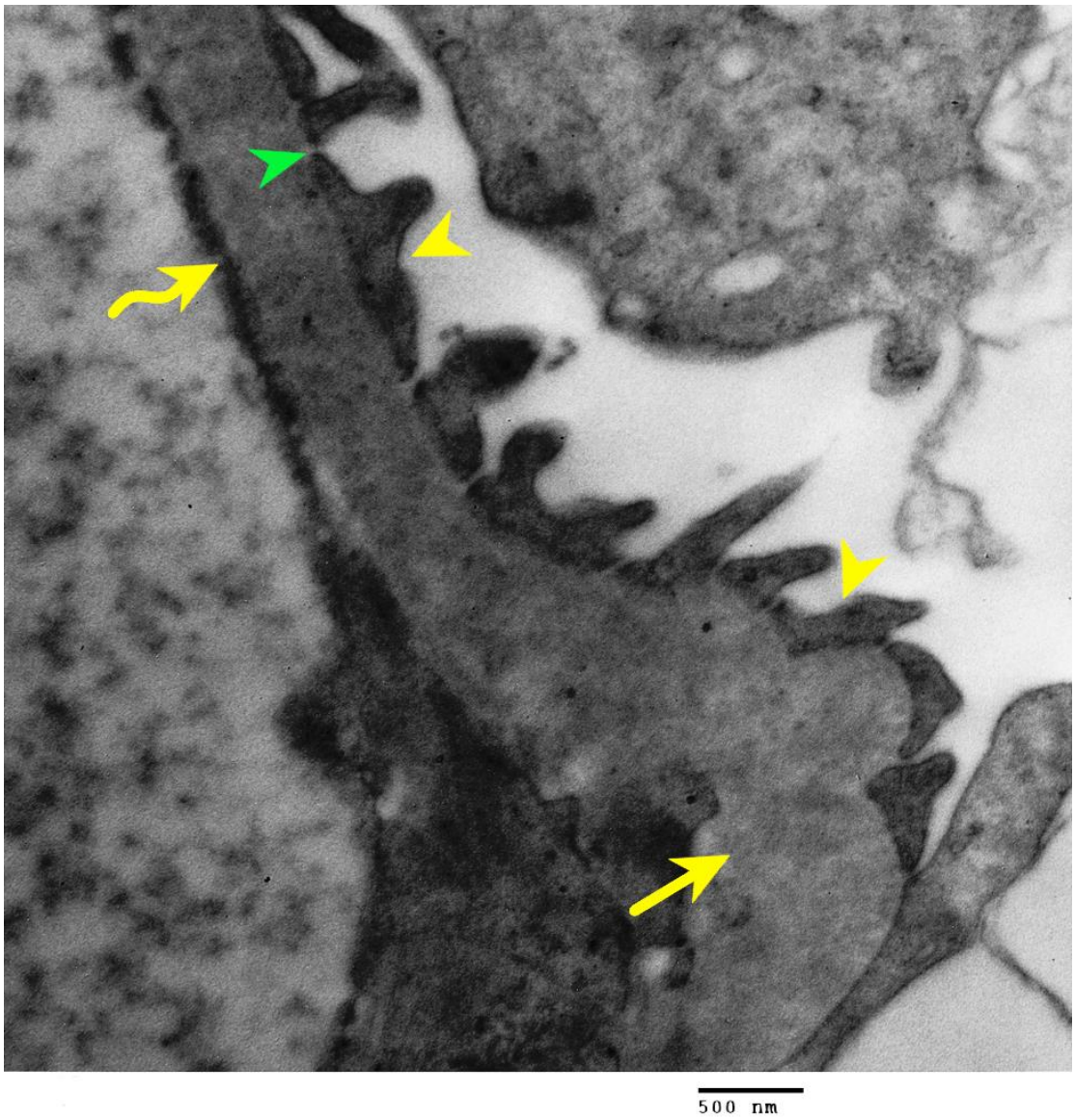

Figure 13: Transmission electron micrograph of PCT from kidney section of Dio group, illustrating cuboidal cells resting on regular basal lamina (curved arrow) with euchromatic nucleus (N). Luminal border microvilli (arrow) showed large area of loss. Vacuolated cytoplasm (star) with many normal mitochondria (m) can be seen. Also, some mitochondria are partially destructed (circle). Notice, intact junctional complex between the cells (head arrow). **(electron microscopy, x 1500)**

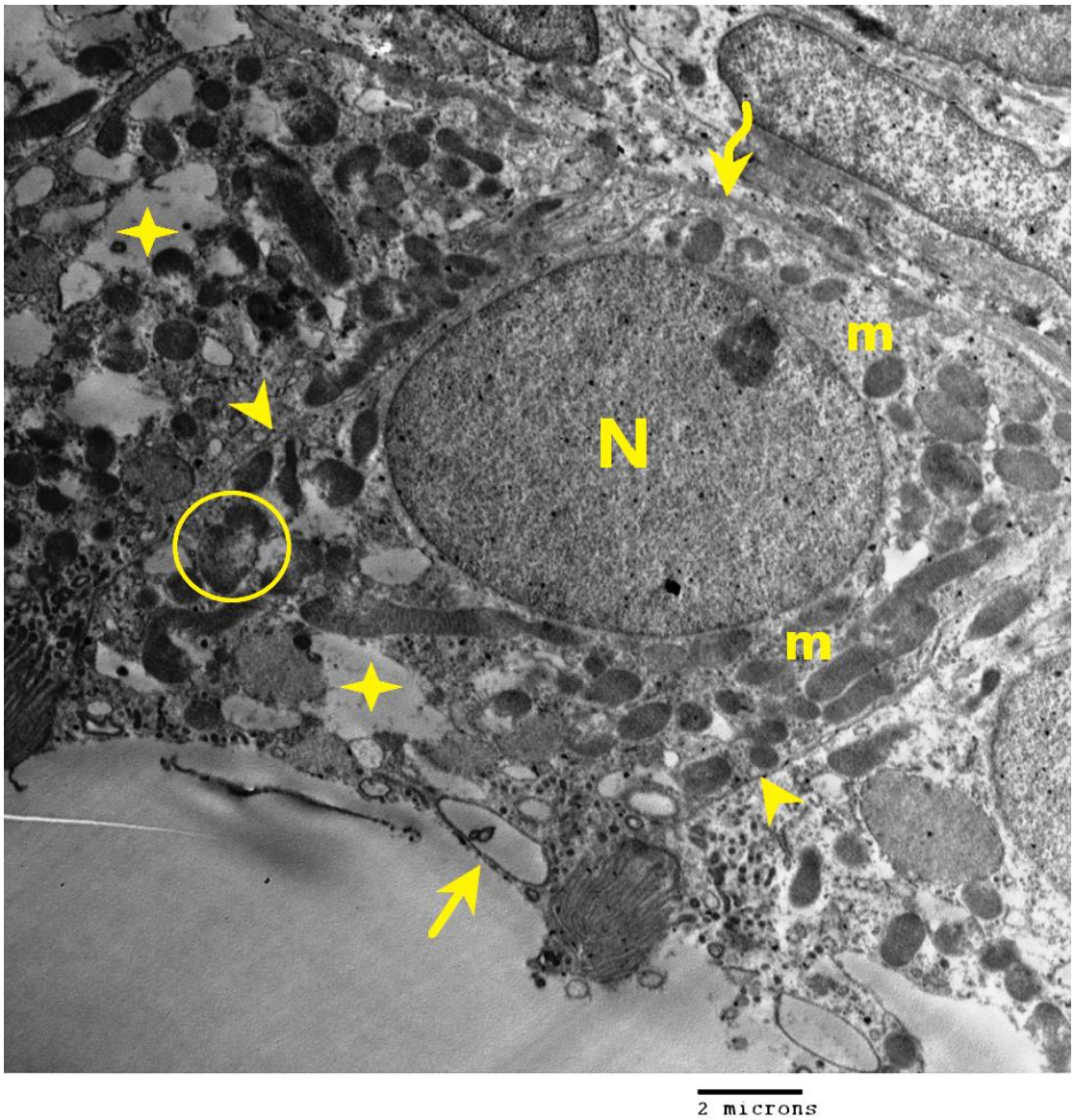

Figure 14: Transmission electron micrograph of DCT from Dio group, illustrating cuboidal cells resting on destructed basal lamina (curved arrow) with extended chromatin of its round nucleus (N). The luminal border has few apical short microvilli (arrow) with area of focal loss. Plentiful scattered mitochondria (m) are observed. Cytoplasmic vacuoles (star) are seen. **(electron microscopy, x 1500)**

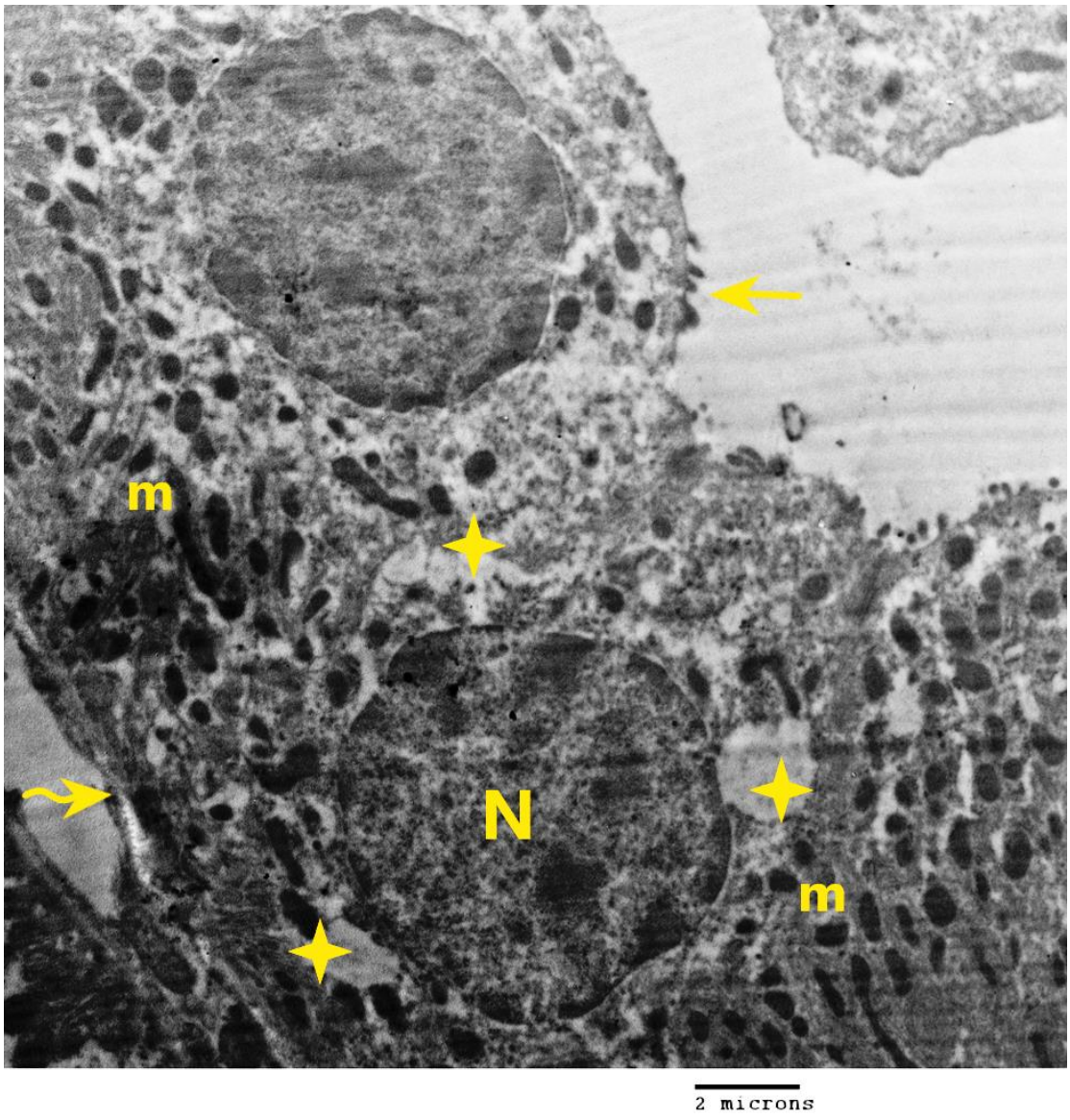

Figure 15: Transmission electron micrograph of kidney section from Gin group, illustrating fenestrae of capillary endothelium (curved arrow). GBM (arrow) appears homogenous and minimally thickened. Some of the secondary foot process appear interdigitating and separated by narrow filtration slits (green head arrow). Few secondary foot processes show effacement (yellow head arrow). **(electron microscopy, x 6000)**

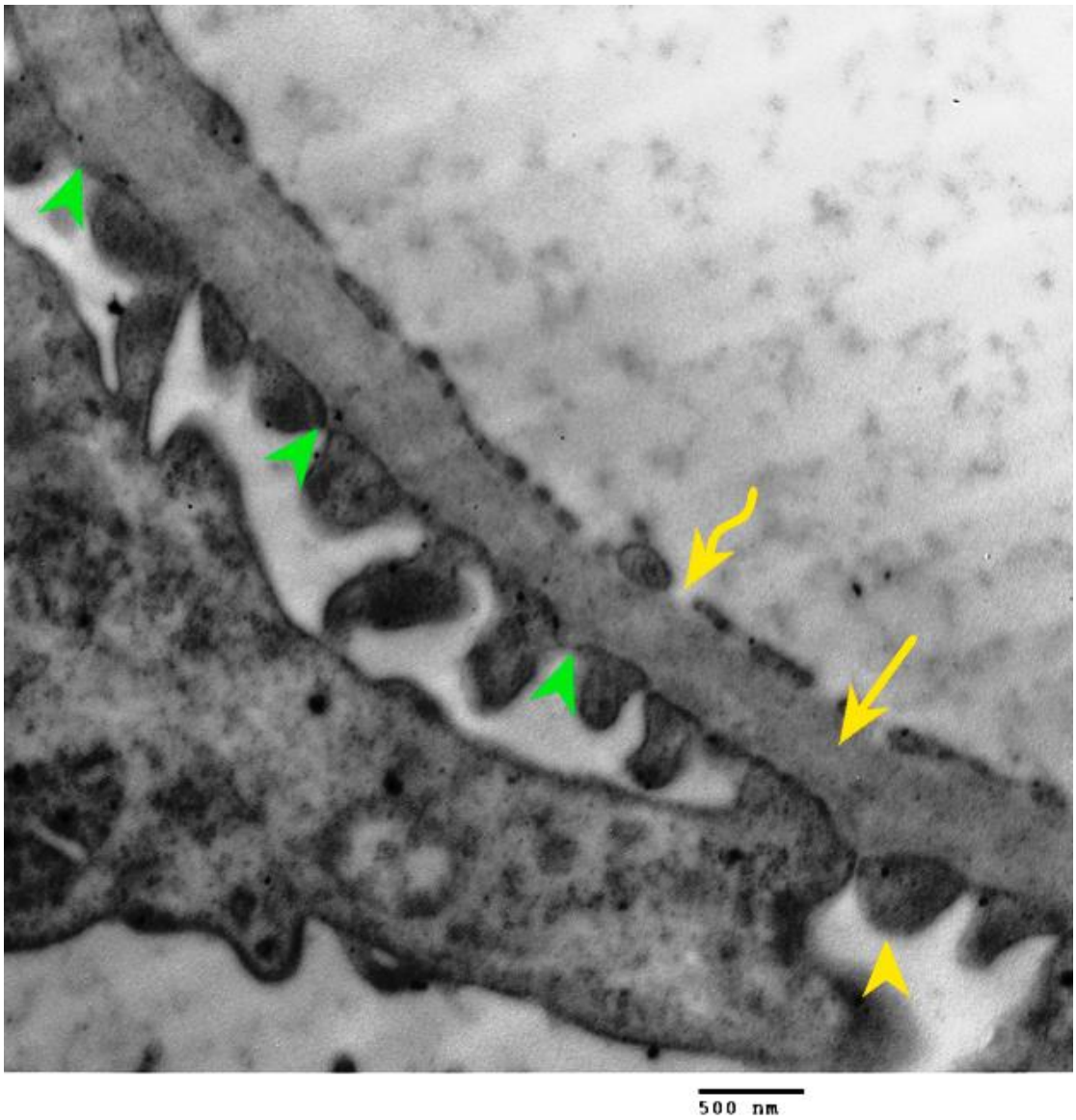

Figure 16: Transmission electron micrograph of PCT from kidney section of Gin group, illustrating cuboidal cells lying down on regular basal lamina (curved arrow) with euchromatic round nucleus (N). The luminal border has apical microvilli (arrow) with area of focal loss. The cytoplasm has long mitochondria (m), lysosomes (L) and few vacuolations (star). **(electron microscopy, x 1500)**

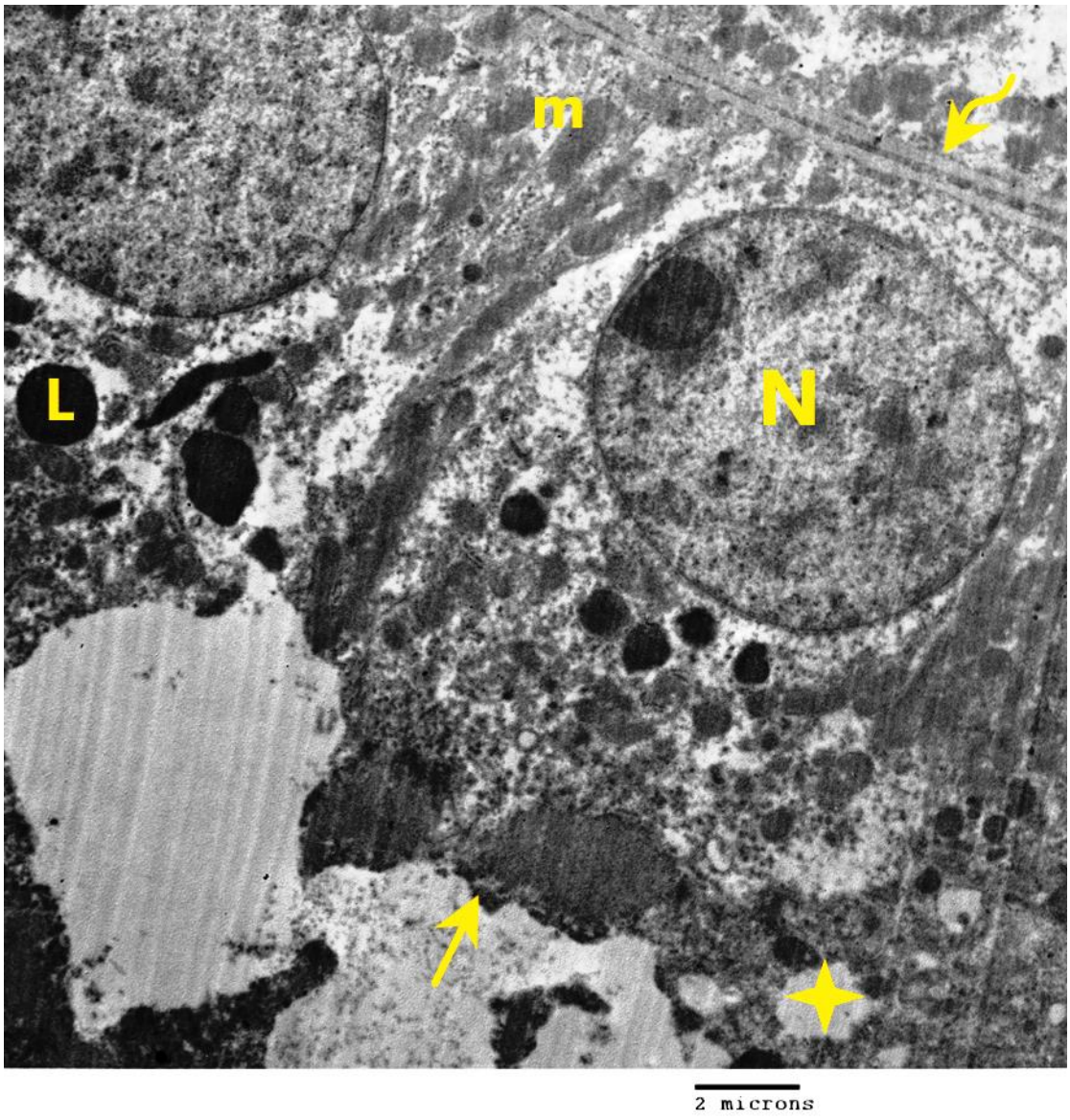

Figure 17: Transmission electron micrograph of DCT from Gin group, illustrating tall cuboidal cells with irregular euchromatic nucleus (N); resting on thin basal lamina (curved arrow). Apical short microvilli (arrow) are present. Basal folding with mitochondria (m) is observed. Notice, intact junctional complex between the cells (head arrow). **(electron microscopy, x 1500)**

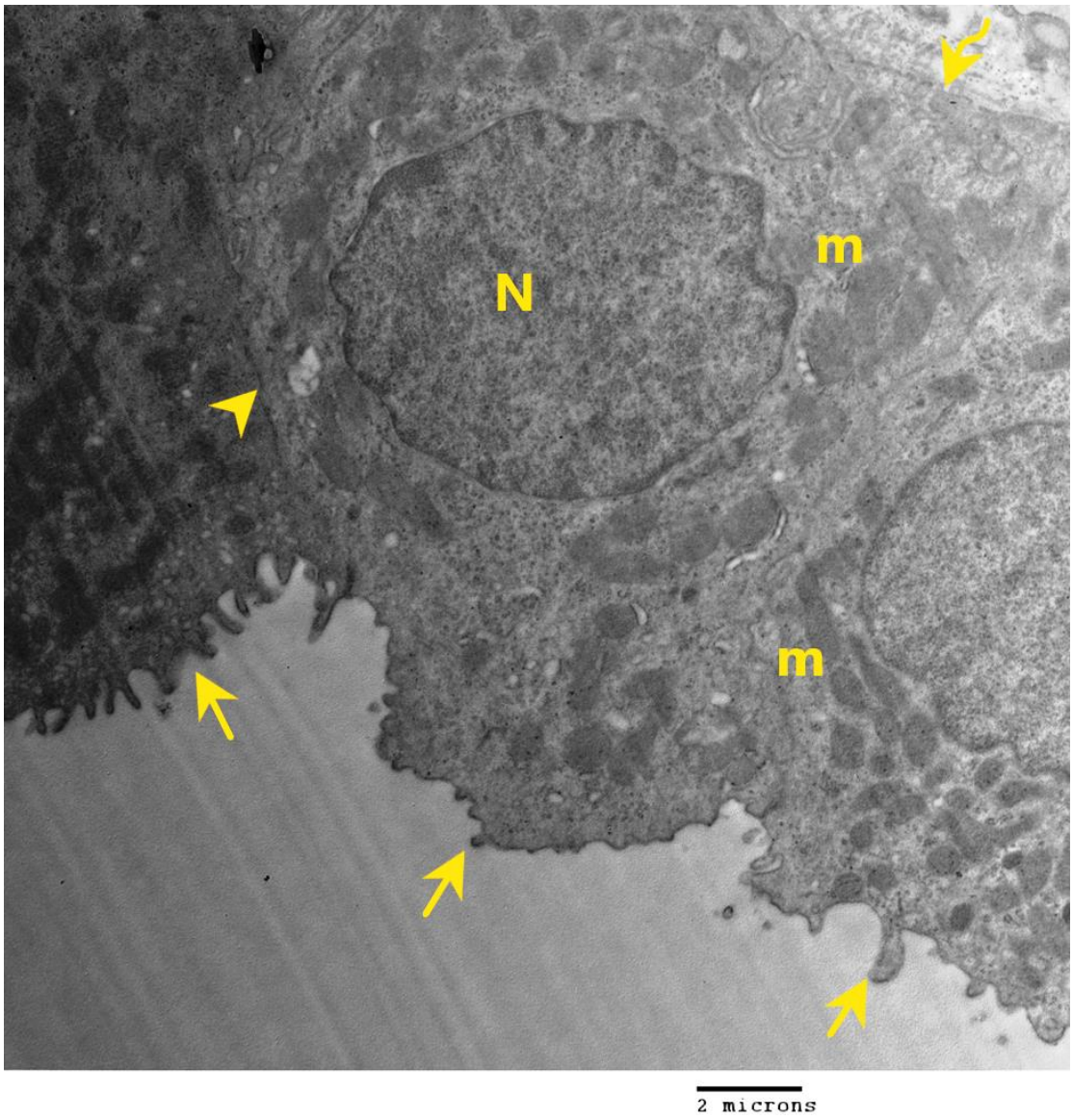

Figure 18: Transmission electron micrograph of kidney section from D+G group, illustrating fenestrae of capillary endothelium (curved arrow). Podocyte with euchromatic nucleus (N) sits on uniform homogenous glomerular basement membrane (arrow). The secondary foot processes (yellow head arrow) appear regularly with filtration slit (green head arrow) in between. **(electron microscopy, x 6000)**

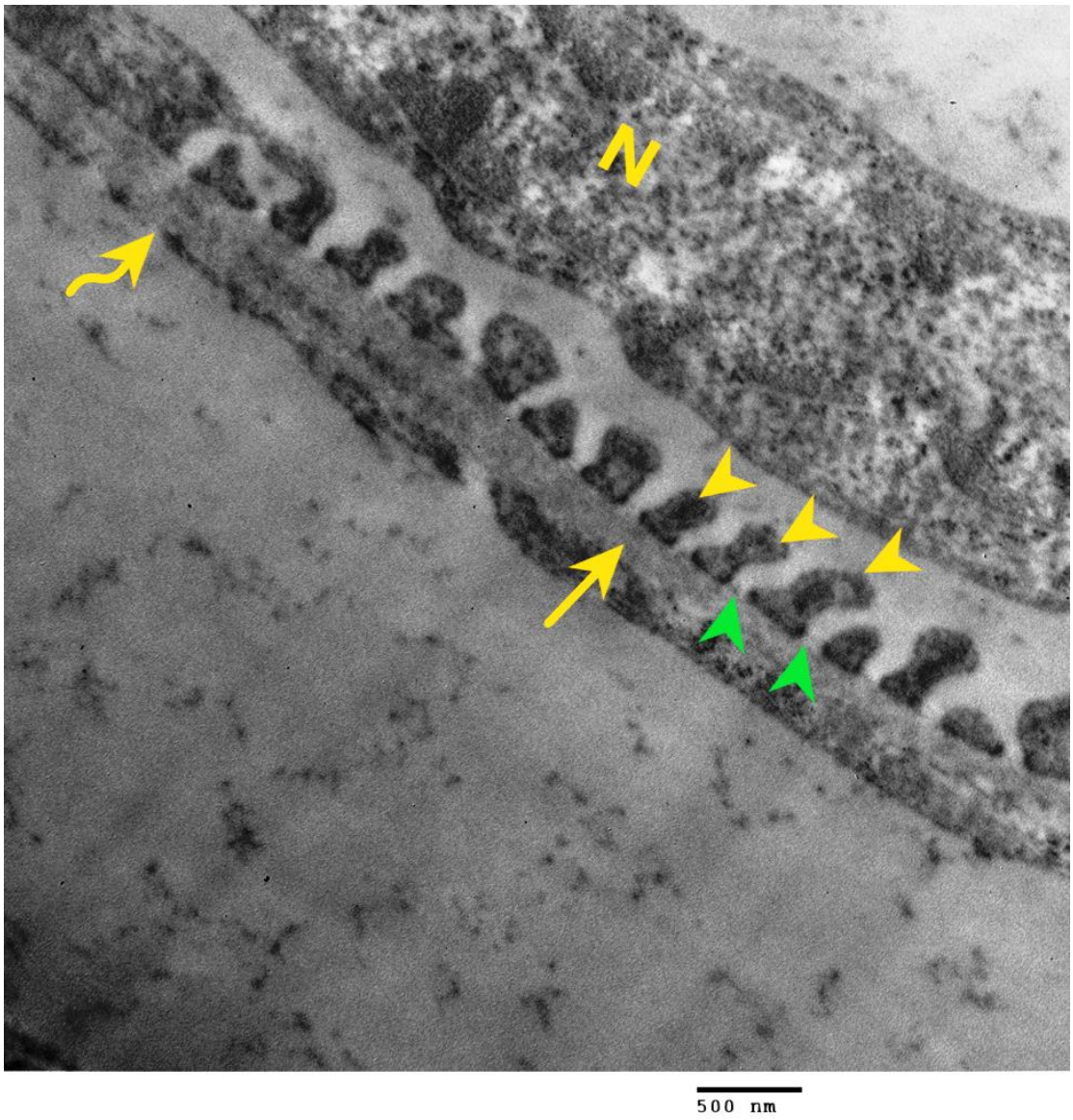

Figure 19: Transmission electron micrograph of PCT from kidney section of Gin group, illustrating virtually normal ultrastructure. The cells of PCT are cuboidal in shape lying down on regular basal lamina (curved arrow) with euchromatic round nucleus (N). The luminal border has tall apical microvilli (arrow) with small area of focal loss (thick arrow). The cytoplasm shows few vacuoles (star). Mitochondria (head arrow) and lipid droplets (i) can be observed. Notice, intact junctional complex between the cells (head arrow). **(electron microscopy, x 1500)**

+

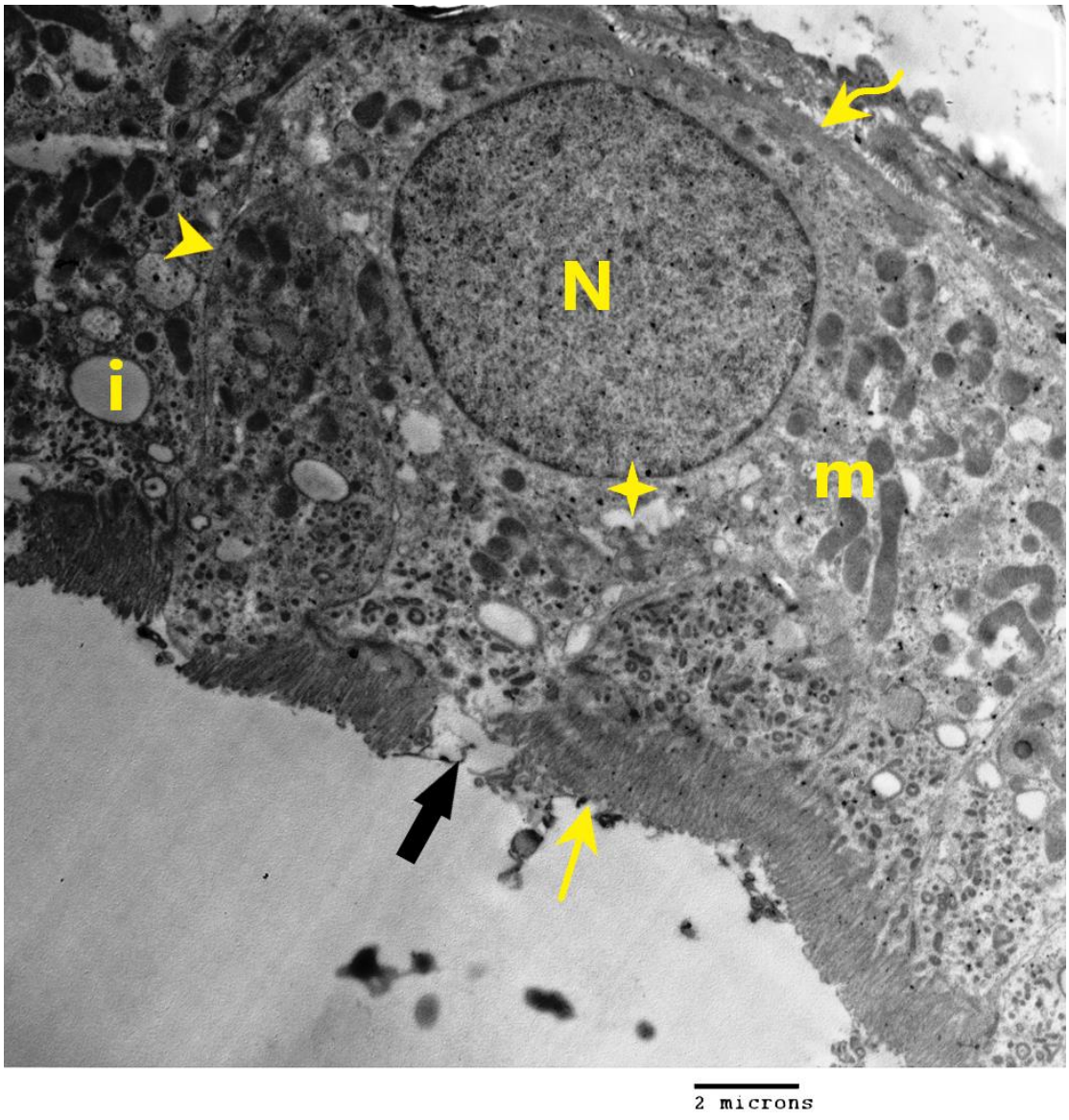

Figure 20: Transmission electron micrograph of DCT from D+G group, illustrating cuboidal cells lying down on on regular basal lamina (curved arrow). Nucleus (N) is nearly round with normal chromatin. Apical short microvilli can be seen (arrow) Mitochondria (m) are occupying basal infoldings. Notice, intact junctional complex between the cells (head arrow). **(electron microscopy, x 1500)**

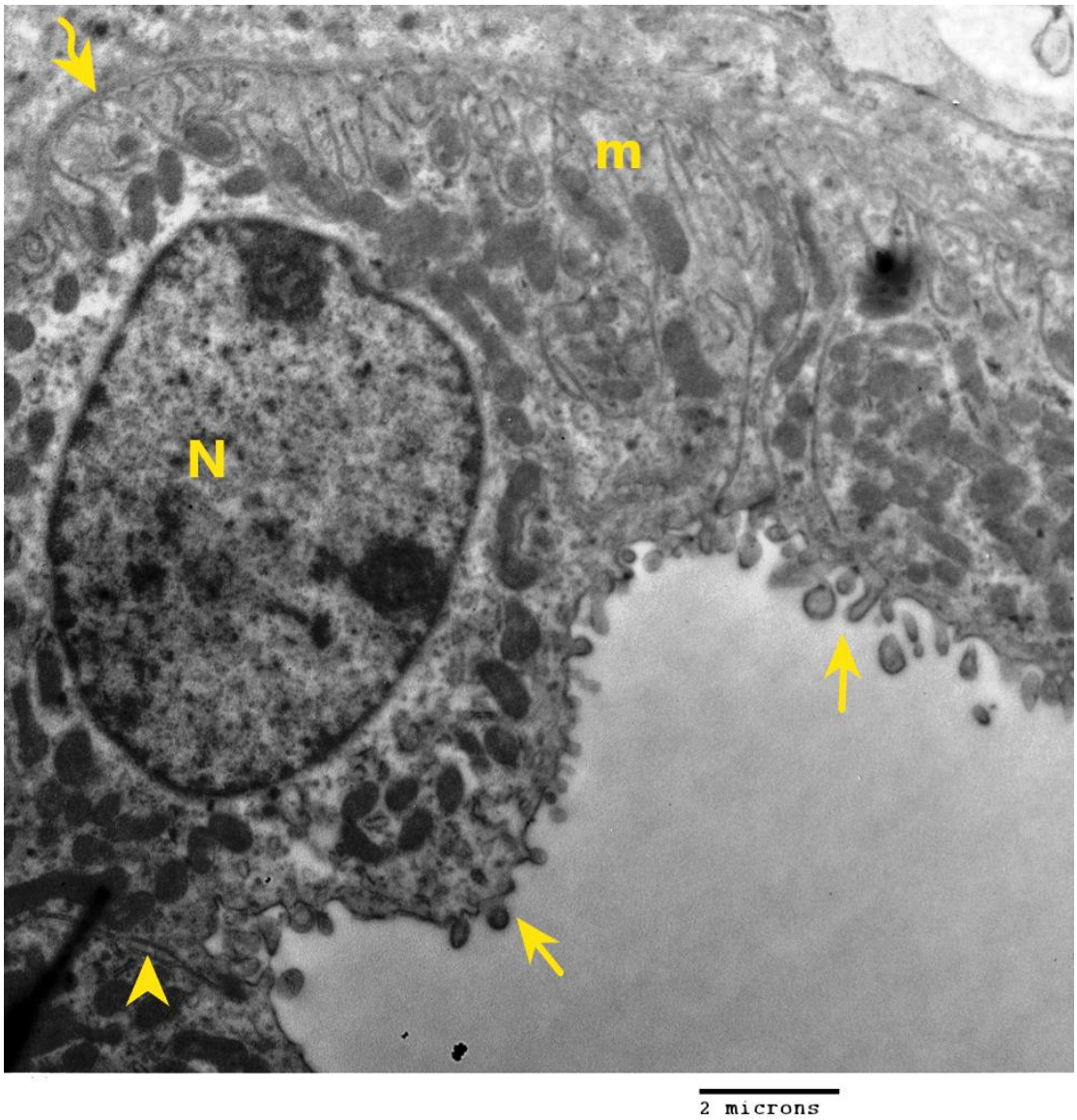

Figure 21: A photomicrograph in kidney sections stained (a–e) with anti Desmin antibodies: (a) control group showing, minimal positive reaction (brown color) of glomerular podocytes (arrow). (b) Diabetic group showing, obvious positive immune reaction (dark brown) of glomerular podocytes (arrow). Dio group (c) and Gin group (d) showing, less obvious positive immune reaction (brown color) of glomerular podocytes (arrow). D+G group (e) showing, minimal positive immune reaction (brown color) of glomerular podocytes (arrow). **(Desmin X400)**

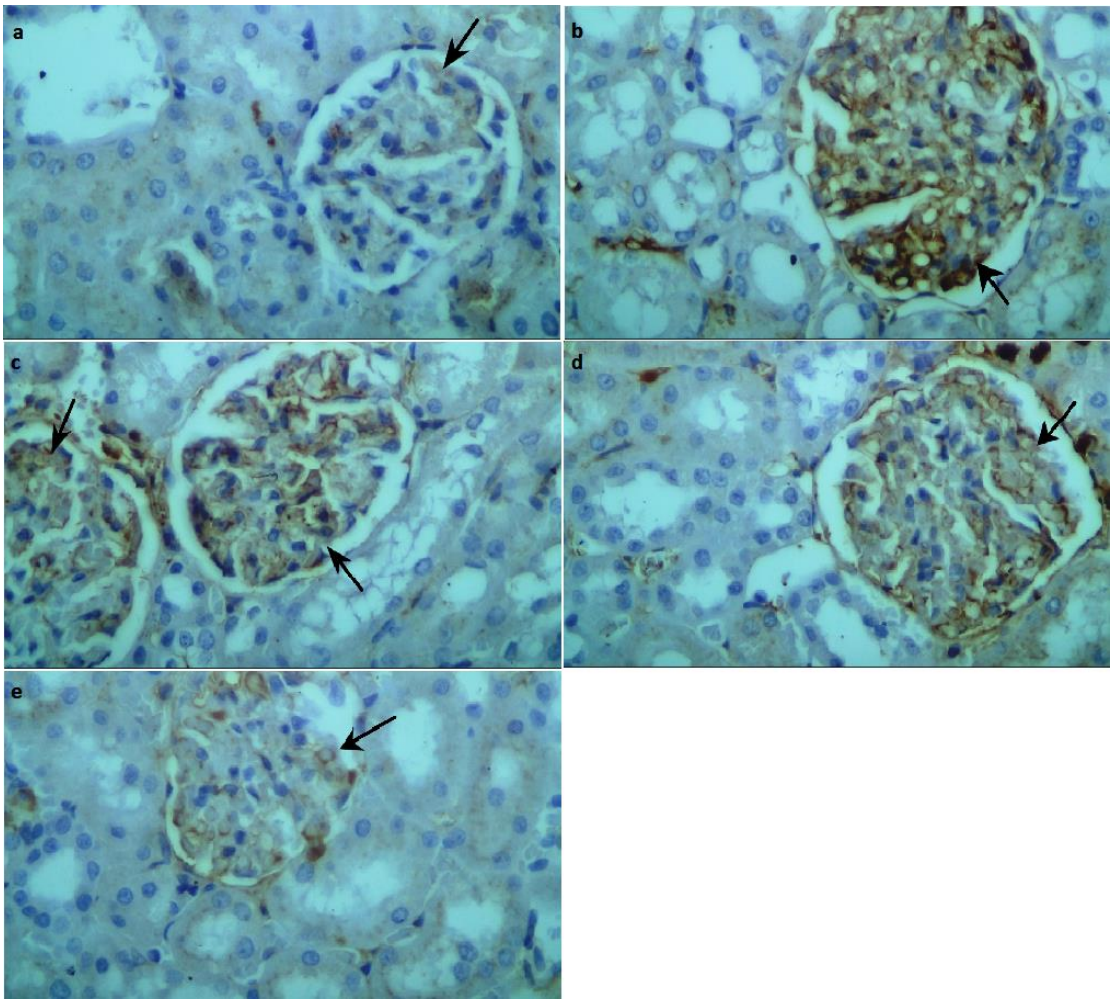

Figure 22: A photomicrograph in kidney sections stained (a–e) with anti Nrf2 antibodies: (a) control group: showing less obvious expression (brown color) in cytoplasm of renal tubules (arrows). (b) Diabetic group: are showing minimal expression (arrows) in cytoplasm of most cells. (c, d) Dio and Gin group respectively: showing increase reaction in the cytoplasm of renal tubular cells (arrows). (e) D+G group: showing obvious reaction in the cytoplasm of tubular cells (arrows). **(Anti Nrf2 antibody X400)**

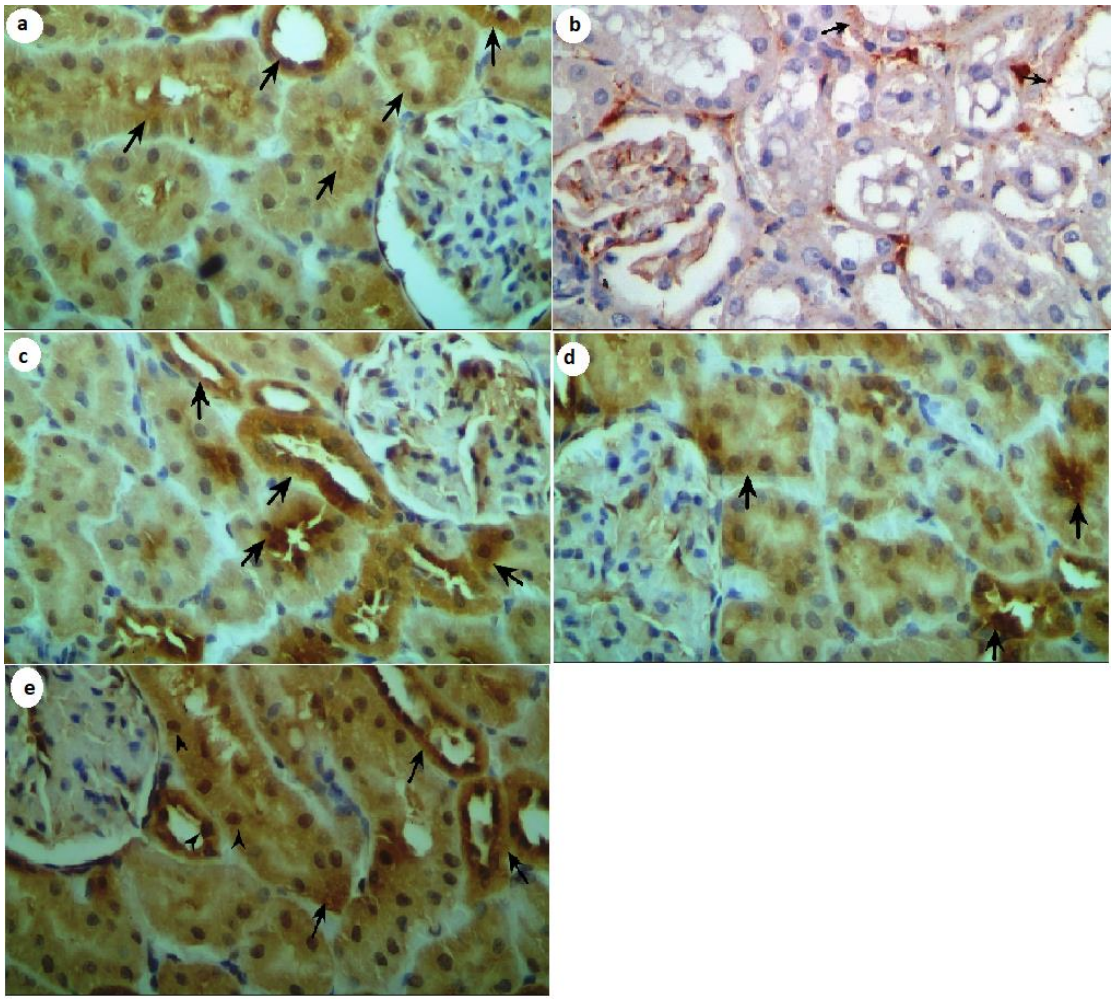

Table 1: ANOVA is used to examine the data, which are shown as Mean values ± SD of the levels of Glucose, urea, and Creatinine in the control and experimental groups. *Significant* (P<0.05) in contrast to other groups

	Control group (n=10)	Diabetic group (n=10)	Dio group (n=10)	Gin group (n=10)	D+G group (n=10)
Glucose (mg/dl)					
Mean ± SD	96.67± 24.58	316 ± 26.51	172.33 ± 4.93	143.67 ± 9.29	130.33 ± 8.96
P 1		**<0.001** [a]	**0.006** [a]	**0.036** [a]	0.090 [ns]
P2			**0.001** [b]	**<0.001** [b]	**<0.001** [b]
P3				**0.009** [c]	**0.002** [c]
P4					0.148 [ns]
Urea (mg/dl)					
Mean ± SD	13.4±0	31.7±0	17.3±0	15.7±0	14.6±0
P 1		**<0.001** [a]	**<0.001** [a]	**<0.001** [a]	**<0.001** [a]
P2			**<0.001** [b]	**<0.001** [b]	**<0.001** [b]
P3				**<0.001** [c]	**<0.001** [c]
P4					**<0.001**[d]
Creatinine (mg/dL)					
Mean ± SD	0.33 ± 0.15	3.2 ± 0.36	1.8 ± 0.26	1.1 ± 0.53	0.77 ± 0.23
P 1		**<0.001**[a]	**0.001** [a]	0.073 [ns]	0.053 [ns]
P2			**0.006**[b]	**0.005** [b]	**0.001** [b]
P3				0.110 [ns]	**0.007** [c]
P4					0.374 [ns]

P1: p value compared to Control group, P2: p value compared to Diabetic group, P3: p value compared to Dio group, p4: p value compared to Gin group,

a: P<0.05 as compared to control group, b: P<0.05 as compared to Diabetic group, c: P<0.05 as compared to Dio group, d: P<0.05 as compared to Gin group, NS: non-significant.

Table 2: ANOVA is used to examine the data, which are shown as Mean values ± SD of the levels of MDA, SOD, and Catalase in the control and experimental groups. *Significant* (P<0.05) in contrast to other groups

	Control group (n=10)	Diabetic group (n=10)	Dio group (n=10)	Gin group (n=10)	D+G group (n=10)
MDA (nmol g protein)					
Mean ± SD	76 ± 1	146.67 ± 23.18	120.33 ± 2.52	107 ± 7	83.33 ± 5.51
P 1		**0.006** [a]	**<0.001** [a]	**0.002** [a]	0.086 [ns]
P2			0.122 [ns]	**0.047** [b]	**0.010** [b]
P3				**0.036** [c]	**<0.001** [c]
P4					**0.010** [d]
SOD (U g protein)					
Mean ± SD	23 ± 2.65	12.9 ± 4.36	19 ± 2	18.11 ± 0.38	15 ± 1
P 1		**0.011** [a]	**0.038** [a]	**0.010** [a]	**0.002** [a]
P2			0.065 [ns]	**0.035** [b]	**0.006** [b]
P3				0.374 [ns]	**0.021** [c]
P4					**0.005** [d]
Catalase (U g protein)					
Mean ± SD	2.13 ± 0.06	0.73 ± 0.59	1.53 ± 0.15	1.87 ± 0.21	2.5 ± 0.4
P 1		**0.015** [a]	**0.003** [a]	0.099 [ns]	0.191 [ns]
P2			0.084 [ns]	**0.034** [b]	**0.013** [b]
P3				0.089 [ns]	**0.017** [c]
P4					0.072 [ns]

P1: p value compared to Control group, P2: p value compared to Diabetic group, P3: p value compared to Dio group, p4: p value compared to Gin group.

a: P<0.05 as compared to Control group, b: P<0.05 as compared to Diabetic group, c: P<0.05 as compared to Dio group, d: P<0.05 as compared to Gin group, NS: non-significant.

Table 1: ANOVA is used to examine the data, which are shown as Mean values ± SD of Area % of Desmin and Area % of Nrf2 in the control and experimental groups. *Significant* (P<0.05) in contrast to other groups

	Control group (n=10)	Diabetic group (n=10)	Dio group (n=10)	Gin group (n=10)	D+G group (n=10)
Area % of Desmin					
Mean ± SD	2.8 ± 0.62	16.3 ± 0.95	8.5 ± 0.61	7.8 ± 0.44	4.4 ± 0.85
P 1		**<0.001 [a]**	**<0.001 [a]**	**<0.001 [a]**	0.059 [ns]
P2			**<0.001 [b]**	**<0.001 [b]**	**<0.001 [b]**
P3				0.181 [ns]	**0.002 [c]**
P4					**0.004 [d]**
Area % of Nrf2					
Mean ± SD	13.13 ± 0.91	3.43 ± 0.5	9.83 ± 1.52	11.7 ± 0.8	16.1 ± 1.73
P 1		**<0.001 [a]**	**0.032 [a]**	0.109 [ns]	0.059 [ns]
P2			**0.002 [b]**	**<0.001 [b]**	**<0.001 [b]**
P3				0.133 [ns]	**0.009 [c]**
P4					**0.016 [d]**

P1: p value compared to Control group, P2: p value compared to Diabetic group, P3: p value compared to Dio group, p4: p value compared to Gin group.

a: P<0.05 as compared to control group, b: P<0.05 as compared to Diabetic group, c: P<0.05 as compared to Dio group, d: P<0.05 as compared to Gin group, NS: non-significant.